An Analytical Framework for Power Quality Monitoring in Smart Power Microgrid

by

Sardar Ali
MS(IT), National University of Sciences and Technology, Pakistan, 2009
BS(IT), Kohat University of Science and Technology, Pakistan 2006

A Dissertation Submitted in Partial Fulfillment of the
Requirements for the Degree of

DOCTOR OF PHILOSOPHY

in the Department of Computer Science

An Analytical Framework for Power Quality Monitoring in Smart Power Microgrid

by

Sardar Ali
MS(IT), National University of Sciences and Technology, Pakistan, 2009
BS(IT), Kohat University of Science and Technology, Pakistan 2006

Supervisory Committee

Dr. Kui Wu, Supervisor
(Department of Computer Science, University of Victoria)

Dr. Dimitri Marinakis, Departmental Member
(Department of Computer Science, University of Victoria, Canada.)

Dr. Hong-Chuan Yang, External Member
(Department of Electrical & Computer Engineering, University of Victoria, Canada.)

ABSTRACT

Due to the high measuring cost, the monitoring of power quality is non-trivial. This work is aimed at reducing the cost of power quality monitoring in power networks. Using a real-world power quality dataset, this work adopts a learn-from-data approach to obtain a device latent feature model, which captures the device behavior as a power quality transition function. With the latent feature model, the power network could be modeled, in analogy, as a data-driven network, which presents the opportunity to use the well-investigated network monitoring and data estimation algorithms to solve the network quality monitoring problem in power grid. Based on this network model, algorithms are proposed to: 1) intelligently place measurement devices on suitable power links to reduce the uncertainty of power quality estimation on unmonitored power links, 2) estimate the power quality in unmonitored segments of a power network, using only a small number of measurement points, and 3) identify a potential malfunction device in the network.

The meter placement algorithms use entropy-based measurements and Bayesian network models to identify the most suitable power links for power quality meter placement. Evaluation results on various simulated networks including IEEE distribution test feeder system show that the meter placement solution is efficient, and has the potential to significantly reduce the uncertainty of power quality values on unmonitored power links. After deploying power quality meters on selected links, a maximum entropy (MaxEnt) based approach is presented to estimate the power quality on the unmonitored lines. Compared to other existing methods such as Monte Carlo Expectation Maximization (MCEM), the MaxEnt based approach is much faster. Finally, using readings from our metered locations, we propose a prediction model that derives an acceptable device behavior to identify a potential malfunction device in the power grid. Our simulation results show that our model accurately detects the malfunction devices and can be used to make proper recommendations of device maintenance and replacement.

Contents

List of Tables

List of Figures

ACKNOWLEDGEMENTS

First and foremost, I am immensely thankful to Almighty *Allah* for letting me pursue and fulfill my dreams. Nothing could have been possible without His blessings.

I would like to thank my *parents* for their continuous support throughout my educational career. They have always supported and encouraged me to do my best in all matters of life.

My wife *Najma*, for dedicating every moment to my happiness and prioritizing my dreams. Her unending love, delicious food, and extended support in the last year of my PhD contributed to the realization of this work.

My heartfelt thanks to my committee members *Dr. Dimitri Marinakis*, and *Dr. Hong-Chuan Yang*, project fellow *Kyle Weston*; and all others who contributed in any way towards the successful completion of this work.

Finally, this thesis would not have been possible without the expert guidance and support of my thesis adviser, *Dr. Kui Wu*, who has been a constant source of knowledge, inspiration, and motivation for me during these years of research. Despite all the assistance provided by *Dr. Kui Wu* and others, I alone remain responsible for any errors or omissions which may unwittingly remain.

Sardar Ali

DEDICATION

To my parents *Subhania* and *Abdulkabir* for their sacrifices, prayers, and support; wife *Najma Bibi* for convencing her parents to marry a PhD student; and our little princess *Manhaa*, who just arrived in the final phase of this writing to give it a final push.

Chapter 1

Introduction

1.1 Why Power Quality Monitoring?

Electrical power networks are one of the critical infrastructures of our society. Due to our high dependence on electricity, the issue of reliability in electric networks has become a core research interest in the area of smart grid [3]. Reliability evaluation of power grid, however, is challenging due to the existence of multiple electric utilities and the potential of cascading failures of power distribution systems [4]. One of the most influential factors impacting the reliability and energy saving of power networks is the power quality delivered to, and experienced by, critical electric equipment. Poor power quality, such as voltage sags/swells, harmonics, fast impulses etc, may lead to power outage and service interruptions. Service unavailability caused by power losses is a serious problem for many companies and organizations, e.g., it may result in a significant revenue loss for Internet service providers or even loss of lives in hospitals. To improve the reliability of power networks, organizations and large companies (e.g., Google data centers) adopt smart microgrid, and closely monitor the power quality in different segments of the microgrid. Hence, the monitoring of power quality is a crucial component of assessing and maintaining reliability in power grids.

Monitoring power quality, however, is not an easy task. Since the power measurement devices [5, 6] are expensive, it is financially impractical to monitor every segment of a power network. The overhead of interconnecting these power meters and developing the power management system further increases the cost. In addition, in many cases direct monitoring of power quality is difficult, e.g., it is hard to install smart meters after power lines were sealed in hard-to-reach areas in a building. We

identify various research challenges in power quality monitoring.

1.2 Open Challenges

In order to effectively monitor the power quality in the smart grid, this work is intended to tackle the following challenges:

1. Based on a limited small number of monitored points in a power network, how can we effectively estimate the power quality of other unmonitored segments of the network?

2. Given a fixed number of available power meters, which grid segments should be selected for monitoring such that power quality can be inferred as accurately as possible in the remaining unmonitored segments of the network? A relevant research problem is to design a mechanism that calculates the optimal number of meters required to achieve an acceptable level of network reliability.

3. Based on readings from our meters installed in the power grid, how can we accurately detect a potential malfunction device?

As the first step to tackle the above challenges, the probabilistic calculation of power quality values on unmonitored links requires the behavior (latent feature) of each device to be known. We represent the latent feature of a device as a transfer function which is usually estimated through physical modeling or through the assessment of historical power monitoring data. Using a real power quality dataset, we show that historical data can be used to capture the latent features of a device. Our device latent feature model is presented in Chapter 3.

With devices' latent features captured, we in the second step introduce a network model of the smart microgid as a data-driven network, in analogy, where we represent the electrical components as network nodes, power links as data links, flow of power as data flow on the links, and the power flowing through links as numeric data. The power quality estimation problem can then be modeled as an optimization problem of missing data estimation in a data network. This problem transformation significantly simplifies the complexity of the power grid network; it also gives us the opportunity to use the well-investigated network monitoring and data estimation algorithms to solve the network quality monitoring in power grids. Chapter 4 presents the proposed network model.

Finally, using our network model, we propose various algorithms to tackle the three challenges we identified in this section. In the next section, we detail the identified challenges and summarize the solutions we propose to solve each challenge.

1.3 Proposed Solutions

Power quality meters play an important role in the reliability evaluations of the power grids. In this thesis, we identify three research problems related to smart meter placement, power quality estimation on unmonitored segments, and detection of a malfunction device in the power grid. Summary of the our proposed solutions for the three research challenges is as follows:

1.3.1 Power Quality Estimation using Maximum-Entropy Approach

The reliability evaluation of enterprise-level power microgrid seems to be much simpler compared to the large-scale power grid which is notoriously difficult due to the existence of the multiple electric utilities and the cascading failures of power distribution systems [4]. Nevertheless, to tackle the practical challenges, the power quality and operational status of electric devices in the micogrid must be monitored and recorded. On the other hand, due to financial and other practical issues, not all devices in the network can be monitored. We need to tackle the following challenge: *Based on a limited small number of monitored points in a power network, how can we effectively estimate the power quality of other unmonitored segments of the network?*

We propose to use a Maximum-Entropy (MaxEnt) [7] approach to power quality estimation. The basic idea of MaxEnt is that out of all probability distributions consistent with a given set of constraints, we should choose the one that has the maximum uncertainty to be the estimated power quality values. Intuitively, the principle of MaxEnt implies that we should make use of all the information that is given and avoid making (biased) assumptions about information that is not available.

The MaxEnt approach is built on the top of our network model which gives us the opportunity to use existing data estimation techniques used in the data networks. The problem of estimating power quality is modeled in such a way where we effectively get the benefit of MaxEnt approach to correctly estimate the power quality values at unmonitored links. We solve the formulated MaxEnt problem and validate

its effectiveness and efficiency with a simulated microgrid system. Compared to other existing methods such as Monte Carlo Expectation Maximization (MCEM), the MaxEnt based approach is much faster. The proposed MaxEnt approach is presented in Chapter 5.

1.3.2 Intelligent Meter Placement using Conditional Entropy

Power quality meters are being deployed to monitor the power quality in the power grid network. Power quality meters are expensive devices [5, 6] and it is impractical to monitor the power quality at every segment in the power grid network. Instead, power quality in unmetered grid locations must be inferred given data obtained from the measured locations. The research question arise is *where to place the meters in the power grid network?*

We propose an iterative approach for identifying network segments suitable for power meter placement. During each iteration of the algorithm we identify in a greedy manner the network segment that suffers from the most unpredictable power quality given the meters deployed so far. We then deploy the next power meter at that location.

A relevant challenge here is to identify the optimal number of meters to reduce the uncertainty and hence the overall reliability of the network to an acceptable level. Formally, we tackle the problem of *how to design a mechanism that calculates the optimal number of meters required to reduce the uncertainty of power quality in the power grid to an acceptable level?* We propose to model the above issue as an optimization problem to minimize the number of meters while maintaining the desired level of network reliability.

For above two problems, the detailed problem definitions, the proposed solutions, and results from an experimental study are presented in details in Chapter 6.

1.3.3 Detecting a Malfunction Device using Our Prediction Model

The main objective of this work is to reduce the cost of power quality monitoring while ensuring the reliability of the power grid network. The two research problems discussed above address how to accurately estimate the state of the network. This information could be used to avoid device failures. We need to propose a model that

could accurately detect any significant change in the normal behavior of a device. By doing so, we would be able to raise an alarm and make recommendations for the device maintenance or possible replacement before the device significantly compromise the reliability (in terms of power quality) of the power grid. The research question is: *how to detect a potential malfunction device in the power network based on available PQ readings*.

To address the challenge, using the power quality readings from the monitored links, we propose statistical measures that accurately detect a potential malfunction device in the power network. Our proposed solution and the simulation results of its accuracy evaluations are presented in Chapter 7.

1.4 Contributions

The proposed thesis work investigate various algorithms to tackle our three research challenges in the area of power quality monitoring in power grid. As the first step to tackle the above challenges, we represent a device latent feature model used to capture the behavior of the devices in the power grid. With devices' latent features captured, we in the second step introduce a network model of the smart microgid as a data-driven network. This problem transformation significantly simplifies the complexity of the power grid network; it also give us the opportunity to use the well-investigated network monitoring and data estimation algorithms to solve the network quality monitoring in power grids.

Our latent feature and network models are detailed in separate chapters in this thesis. Using the network model, we propose various algorithms to tackle the three challenges and make the following three major contributions:

1. **Power Quality Estimation:** A Maximum-Entropy (MaxEnt) approach to power quality estimation. The proposed solution is presented in Chapter 5.

2. **Intelligent Meter Placement:** An intelligent entropy-based algorithm and a Bayesian network based approach to solve the meter placement problem. The proposed meter placement algorithms and their detailed evaluations are presented in Chapter 6.

3. **Malfunction Device Detection:** Based on statistical measures, we propose a prediction model to detect a potential malfunction device in the network. Using

the inferred and actual PQ values by meters we placed using our intelligent meter placement algorithms. The proposed model with its simulation results is presented in Chapter 7.

1.5 Thesis Outline

The rest of the thesis is organized as follows. Chapter 2 provides review on power quality in smart grid and discusses the available literature related to our proposed work. The proposed device latent feature model is presented and evaluated on a real dataset in Chapter 3. Our network model of the power grid is presented in Chapter 4. Based on the proposed network model, we build various algorithms to address the identified research issues. The research issue of estimating power quality values on unmonitored links is investigated in Chapter 5. In Chapter 6, we propose algorithms that intelligently place the power meters on high information locations in the power grid. In Chapter 7, based on the known power quality values from our proposing algorithms, we present a prediction model that detects a potential malfunction device. The thesis in concluded and the possible future extensions are discussed in Chapter 8.

Chapter 2

Background and Related Work

Due to our high dependency on electric power, reliability of power networks has become critically important. A variety of hardware and software tools for measuring and monitoring the power quality are available. Before we detail the cutting-edge research work in the area, we first discuss the most important causes of power quality problems.

2.1 Main Causes of Power Quality Problems

2.1.1 Voltage Sags/Swells

The voltage sags are brief reductions in voltage while the voltage swells are brief increase in voltage level which may last for a period of 0.5 cycle to a few seconds. Voltage sags are caused by faults, sudden increases in loads or device impedance, short circuits or faults. Causes of voltage swells are an abrupt reduction in load on a circuit or a damage in neutral connection. Sag or swell is the largest cause of problems from the utility side. Sags or swells can occur in the power distribution network or at the point of use. These types of disturbances can lead to loss of production or electronic device failures. Measurement devices being used should be able to detect these events. A standard reference for measuring the power quality events largely used by industry is the Computer Business Manufacturers Association (CBEMA) also known as ITI Council profile curve [8]. Power quality monitoring devices use the ITI curve as a reference to highlight if the voltage events may result in any potential problem.

2.1.2 Harmonics

A harmonic is a periodic, integer multiple wave of the fundamental frequency. They are caused by non-linear electric loads. Technically, voltage harmonics are caused by the combination of line impedance and current with a frequency other than the fundamental frequency. Harmonics in power grids are the main cause of power quality problems. A lot of harmonics in the power systems can cause malfunctioning or damage to the electric devices. Power quality measurement devices use the technique of Fourier Analysis to detect the magnitude and frequency of voltage harmonics.

2.1.3 Interharmonics

Interharmonics are distortions in the current or voltage wave-forms. They are different from ordinary harmonics in that it refers to voltages or currents having frequency components that are not integer multiple of the fundamental frequency. They can be found in networks of all voltage classes. They can affect power-line carriers, lighting, computer displays, heating of transformers and motors, miss-operation of electronic devices etc. However, due to their small amplitude and uncertain frequency, they are difficult to detect.

2.1.4 Transients

Transients (also known as *surges* or *spikes*) are momentary changes in voltage or current that last for a very short period of time. The interval is usually less than $1/16^{th}$ of a voltage cycle or about 1 milliseconds. The typical duration of voltage transients is 50 microseconds while the duration of current transients is 20 microseconds. Transients can come from external sources as well as from within the system. The external sources include lightning, switching of facility loads, poor or loose connections in the distribution system, opening/closing of disconnects, tap changing on transformers, and environmental changes. The main culprits within the system causing transients include device switching, arcing, static discharge, and adding or removing loads. If left unchecked, transients can lead to device degradation over time.

2.1.5 Other Causes

As discussed earlier, the life time of electric/electronic devices is dependent on the electric power quality. There are many other causes which effect the power quality in

the electric network. In order to improve the reliability of the electric power network, the causes of the power quality problems need to be addressed. Some of the main other causes are as follows.

Over/Undervoltage

When the Root Mean Square (RMS) value of the voltage in a power system raises above 110% for a duration of greater than 1 minute, it is classified as an over-voltage. It happens when the system is either too weak to support the desired voltage or the voltage controls are sufficient. They are usually the result of switching off a large load. The over-voltage is usually protected using bulk capacitors.

An under-voltage is a decrease in the RMS voltage value when it falls under 90% of its original level for a duration of greater than 1 minute as classified by the CBEMA curve [8]. Its causes include overload circuits, load switching, and capacitor bank switching off. Under-voltages may result in premature shutdown of circuits, loss of important data, restart of electronic equipment.

Sustained Interruptions

It is a decrease in the voltage level to zero for a period of more than 1 minute as defined by IEEE standard [2]. They are often permanent in nature which requires manual intervention to restore the system. This type of interruptions are due to permanent faults caused by storms, equipment failures, trees striking lines, and other environmental factors. If not tackled on time, these faults may result in a complete shutdown of the facility.

Voltage Unbalance

It is defined as the largest difference of the RMS voltage value (or phase angles) on a line from its average value. It is quantified in terms of ratios of the negative and zero components to the positive sequence. Voltage unbalance is usually caused by uneven distribution of voltage between the phases of an n-phase (usually 3-phase) system. It may also caused by mismatch of the impedance of a transformer, a blown fuse, or a bad capacitor. The problem may cause premature equipment aging, power supply ripple, insulation degradation, decrease in mean time between failures (MTBF).

Frequency Variations

Frequency variation is the deviation of fundamental frequency from its nominal value. The size and duration of the frequency shift is dependent on the load characteristics. It is usually caused when a large load is disconnected or when a large power generator goes off-line. It can cause data loss, device crash/damage, or erratic operation in the electronic system.

2.2 Classification of Power Quality Disturbances

It is a known phenomena that when a power system is disturbed either by a short circuit, sudden increase in load, or any other relevant cause, the balance of energy is disturbed. During the disturbance, energy exchange between the electric and magnetic fields occurs which deviates the wave-shapes of voltages and currents in the power system. This electromagnetic phenomena is standardized by two leading knowledge bodies in the field by standards: 1) IEC/TS 61000-2-5; and 2) IEEE Std. 1159-1995.

2.2.1 The IEC Classification

The International Electrotechnical Commission (IEC) classifies various phenomena that cause electromagnetic disturbances through their standard IEC/TS 61000-2-5 [1]. These disturbances can reach the equipment either by conductive or radiative coupling pathways. When there is a physical pathway between the source of emission and the affected device, it is a conductive coupling. On the other hand, radiative coupling occurs when there is no physical pathway but the emission propagates through electric and magnetic fields. Based on couplings and relative frequencies of the disturbances, IEC classifies the electromagnetic phenomena into six categories as shown in Table 2.1.

Table 2.1: Electromagnetic Disturbance Phenomena Categories [1]

1. **Conducted low-frequency phenomena**
   - Harmonics, interharmonics
   - signaling systems
   - Voltage fluctuations
   - Voltage dips and interruptions
   - Voltage unbalance
   - Power frequency variations
   - Induced low-frequency voltages
   - DC in AC networks
2. **Radiated low-frequency field phenomena**
   - Magnetic fields
   - Electric field
3. **Conducted high-frequency phenomena**
   - Directly coupled or induced voltages or currents
   - Unidirectional transients
   - Oscillatory transients
4. **Radiated high-frequency field phenomena**
   - Magnetic fields
   - Electric fields
   - Electromagnetic fields
5. **Electrostatic discharge phenomena (ESD)**
6. **High-altitude nuclear electromagnetic pulse (HEMP)**

Table 2.2: Characteristics of the EM phenomena [2].

Categories	Spectral Content	Duration	Voltage Magnitude
1. Transients			
(a) Impulsive			
i. Nanosecond	5-ns rise	< 50 ns	
ii. Microsecond	1-μs rise	50 ns - 1 ms	
iii. Millisecond	0.1-ms rise	> 1 ms	
(b) Oscillatory			
i. Low frequency	< 5 kHz	0.3 – 50 ms	0 – 4 per unit
ii. Medium freq.	5 – 500 kHz	20 μs	0 – 8 pu
iii. High frequency	0.5 – 5 MHz	5 μs	0 – 4 pu
2. Short-duration RMS variations			
(a) Instantaneous			
i. Sag		0.5 – 30 cycles	0.1 – 0.9 pu
ii. Swell		0.5 – 30 cycles	1.1 – 1.8 pu
(b) Momentary			
i. Interruption		0.5 cycles – 3 s	< 0.1 pu
ii. Sag		30 cycles – 3 s	0.1 – 0.9 pu
iii. Swell		30 cycles – 3 s	0.1 – 1.4 pu
(c) Temporary			
i. Interruption		> 3 s – 1 min	< 0.1 pu
ii. Sag		> 3 s – 1 min	0.1 – 0.9 pu
iii. Swell		> 3 s – 1 min	0.1 – 1.2 pu

Continued on next page

Table 2.2 – continued from previous page

Categories	Spectral Content	Duration	Voltage Magnitude
3. Long duration RMS variations			
(a) Interruption, sustained		> 1 min	0.0 pu
(b) Under-voltages		> 1 min	0.8 – 0.9 pu
(c) Over-voltages		> 1 min	1.1 – 1.2 pu
(d) Current overload		> 1 min	
4. Imbalance			
(a) Voltage		steady state	0.5 – 2%
(b) Current		steady state	1.0 – 30%
5. Waveform distortion			
(a) DC offset		steady state	0 – 0.1 %
(b) Harmonics	0 – 9 kHz	steady state	0 – 20 %
(c) Interharmonics	0 – 9 kHz	steady state	0 – 2 %
(d) Notching		steady state	
(e) Noise	broadband	steady state	0 – 1 %
6. Voltage fluctuations	< 25 Hz	intermittent	0.1 – 7 %
7. Power frequency variations		< 10 s	$\pm$ 0.10 Hz

2.2.2 The IEEE Classification

The Institute of Electrical and Electronics Engineers (IEEE) puts efforts to standardize power quality terminology to allow the parties involved in to have standard and consistent terms. The IEEE standard 1159-1995 [2] provides a classification of power quality events. The various power quality events are classified into seven general categories. The classification is based on event characteristics such as spectral content, duration, and magnitude as shown in Table 2.2.

2.3 Related Work

Power quality is a crucial component of power system reliability. Poor power quality may lead to service interruptions. To improve the reliability of power grid networks, power quality measurement devices are being deployed to closely monitor the power quality on underlying power links. As discussed, it is not feasible to monitor every segments of the network. Instead we propose to 1) intelligently place the monitoring devices on selected network segments; and 2) estimate the power quality on unmonitored links base on the known information from the monitored links.

We also address the relevant research problems such as 1) how many meters are required to achieve the desired level of network reliability; and 2) based on reading from the monitoring devices, how to accurately identify a malfunctioning device that degrades the power quality in the power system. This section covers the research work relevant to our proposed solutions addressing the above identified problems. We classify the existing research (and available techniques) related to this work in the following categories.

2.3.1 Classification of Power Quality Events

There are many approaches to the problem of classifying the power quality events. Typically, power quality is assigned a label based on the magnitude and duration of the electromagnetic phenomena (e.g., voltage sag or swell). Electrical utilities typically report a System Average RMS Variation Frequency Index (SARFI) which is essentially a count of the number of times the magnitude and duration fall below (or above) a threshold. The IEEE and IEC also have their standards for classifying individual power quality events [1, 2]. These standards are detailed in Section 2.2.

We use a discrete classification system in this work, similar to that described in the IEEE standard [2].

2.3.2 Power Reliability

The industry standard practices for electric power reliability in networks focus on measures such as Mean Time Between Failure (MTBF), reliability, and availability as defined by the IEEE Gold Book [9]. These measures are theoretical values, measured or calculated for components and networks operating under standardized conditions. They serve as methods for comparison but are not intended as predictive tools for networks that operate in realistic environments with varying temperature, humidity, load, and power quality.

Further, it is known that there exists a relationship between power quality and the lifetime and performance of components [8]. For an effective evaluation of power reliability, we need to accurately estimate power quality, which motivates the meter placement, and power quality estimation problems studied in this work.

2.3.3 Power Quality Estimation/Improvement

There have been recent studies to improve the electric power quality. In [11], a proactive approach was introduced to identify bad power quality events before they become a concern to end-users. The approach determines voltage threshold limits to determine if a potential voltage problem exists. Another recent study [12] uses Genetic Algorithm (GA) to estimate the harmonic states of the power network. The methodology was shown to be effective for estimating voltage and current state variables. A secondary control scheme is proposed in [13] to enhance the voltage quality of sensitive load bus (SLB) in microgrids. Another recent work [14] proposed a transient state estimator to detect losses due to poor power quality. The estimator was validated on a test system to detect the presence of voltage sag/dip. Another estimator was proposed in [15] that improves the power consistency by identifying angle biases and current scaling errors using phasor-measurement based state estimator (PSE).

We use data estimation techniques to propose our power quality estimation solution (see Chapter 5). A short description of the EM and MaxEnt algorithms used in our work are as follows:

The Expectation Maximization (EM)

EM is a general approach to iterative computation of maximum-likelihood estimates when the observations can be viewed as incomplete data. Since each of the iteration of the algorithm consists of an expectation step followed by a maximization step, the algorithm is named as the EM algorithm. The successive iterations always increase the likelihood and the algorithm converges at a stationary point.

Maximum Entropy (MaxEnt) Estimation

MaxEnt solves convex optimization problems of the form,

$$\textbf{maximize } g(\vec{x}) = -\sum_{i=1}^{n} x_i \log x_i$$

$$\text{subject to } \mathbf{A}\vec{x} \leq \mathbf{c},\ \mathbf{B}\vec{x} = \mathbf{1},$$

where $\vec{x} \in \mathbb{R}^n$ is the optimization variable, $A \in \mathbb{R}^{m \times n}$, and $B \in \mathbb{R}^{m \times n}$ are problem parameters; and $\mathbf{1}$ is a vector with all 1's.

2.3.4 Meter Placement

There is a great body of work on the optimal sensor deployment problem [16]. The meaning of sensors is broad, including any measurement/monitoring devices. In the context of power networks, optimal deployment of phasor measurement units (PMU) has been studied [17].

Another work [18] shows that adding few extra PMUs could improve the bad data detection in the network state estimation. A relevant work addressing the problem of distribution system state estimation (DSSE) was proposed [19] to minimize the state estimation errors. The optimal PMU placement and its communication infrastructure was designed [20] to address the problem of state estimation. A procedure finding the optimal trade-offs between PMUs and metering devices for distribution state estimation was investigated in [21]. Nevertheless, we have not seen any work on studying optimal meter placement problem in the context of network-wide power quality estimation. Further, there are three major differences between the existing PMU placement algorithms and our algorithm.

1. We focus on distribution networks at the enterprise level (e.g., a university campus).

2. Our method is data driven and is based on statistical machine learning method.

3. The existing PMU placement algorithms address the problem of estimating network states and do not consider power quality estimation explicitly.

2.3.5 Bayesian Inference

We use Bayesian inference to identify high information locations for deploying smart meters (detailed in Chapter 6). The Bayesian inference methods are helpful in providing the new estimates of the PQ values on unmonitored links given evidences obtained from the metered locations. Bayesian inference is a general and well-investigated discipline which has applications in a wide range of fields. Several algorithms are available to address specific problem in this domain. For the problem of meter placement, several message passing algorithms could be used to help determine the optimal meter placement. We chose the belief propagation or sum-product algorithm [22] since it is well understood, has been shown to work for general topologies [23] including tree networks, and has software libraries available to the public.

Chapter 3

Capturing the Latent Features of Power Devices

3.1 Introduction

The objective of this work is to reduce the cost of power quality monitoring by intelligently placing power quality meters on selected links in the power network. After deploying limited number of meters, we should be able to estimate the power quality (PQ) values on unmonitored links as accurately as possible. A candidate link for meter placement is the one whose power quality is the most uncertain. The challenge here is how to identify the most uncertain links. Clearly, the PQ values on any power link are dependent on the physical characteristics of the electric devices. For example, the power quality at the output link of a UPS is more predictable than that of a switch. Hence, we need to know the behavior of each device in the network. We call the behavior of a device its latent feature or simply a transition function, which is usually estimated through physical modeling or through the assessment of historical power monitoring data.

In this chapter, we first introduce a latent feature model to capture the behavior of electric devices in the power network. Using a real power quality dataset, we then demonstrate that the historical data can be used to capture the latent features of a device. We use k-fold cross-validation technique to measure the accuracy of latent features we obtain using our dataset. Experimental evaluations show that the captured latent features are consistent. The latent features (or transition functions) are then used to propose our meter placement algorithms.

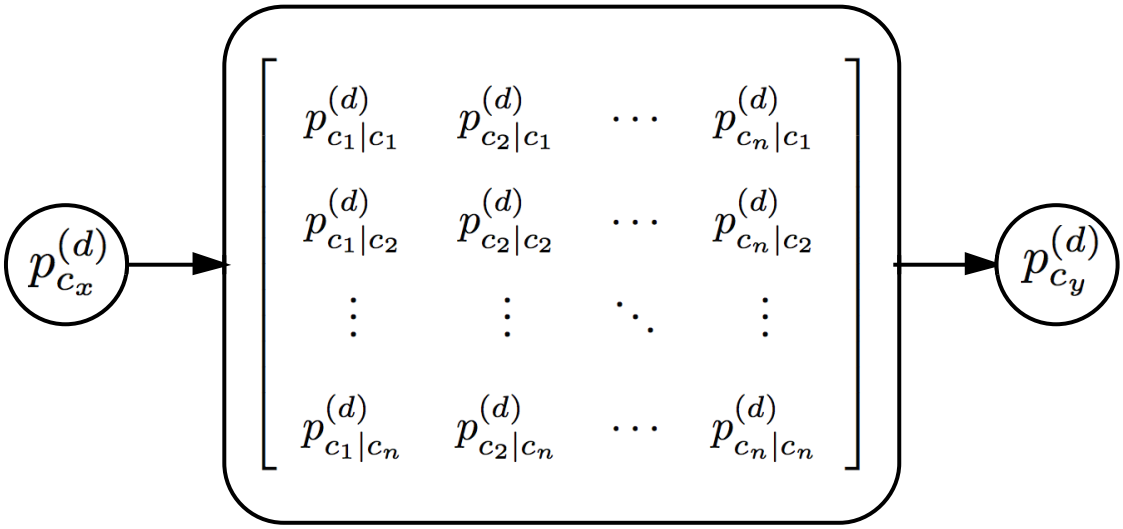

Figure 3.1: Latent feature model of a device d where the two circles represent the power quality meters at input and output of node d; the matrix inside the node d represents the transition function of the node.

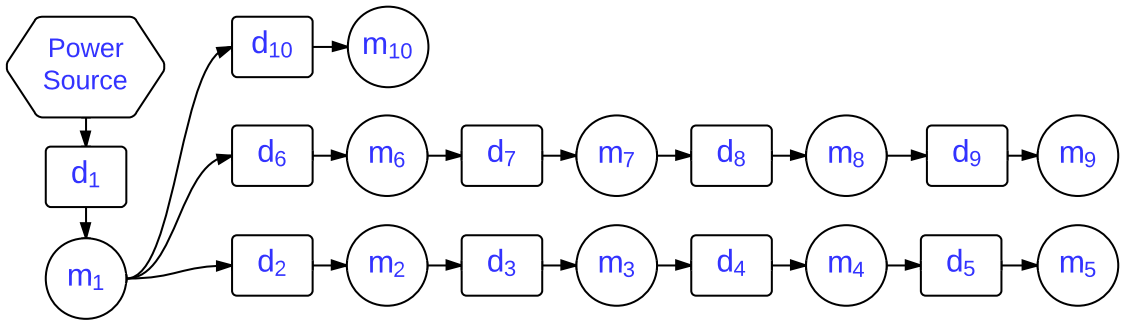

Figure 3.2: Graph network of power quality meters installed in a power network.

3.2 The Latent Feature Model

The latent feature model is basically a mechanism for capturing and mathematically representing the behavior of a device. We capture this behavior by monitoring the input and output links of electric devices and representing it as a transition function. A transition function ($f(d)$) of a device d is the matrix consisting of real values representing the probabilities that a power quality input c_x is mapped to another power quality c_y at the output link of a device d. Figure 3.1 shows the proposed latent feature model we use to capture $f(d)$. We use a real-world power quality dataset collected for a period of over 4 years to capture the latent features of various electric devices. The latent feature $f(d)$ is then used to estimate the power quality at unmonitored power links in the power network.

3.3 Power Quality Dataset

Our power quality dataset was collected at an enterprise power network for a period of four years. For privacy and security reasons, the physical network structure/diagram is omitted. Instead, we represent the topology/positions of the installed power quality meters via a graph network as shown in Fig. 3.2. There are a total of 10 power quality meters (numbered from m_1 to m_{10}) installed. Each meter reported the power quality events (sag/swell, transient, etc.) to the data collection server via Ethernet network. It is important to mention that we currently do not consider power transmission network, which is large-scale and may involve multiple utilities across a country, but only focus on power distribution network at the enterprise-level, e.g., university campus. Hence, we collect the power quality dataset at an enterprise network located at the distribution level. The network is using a standard three-phase distribution system. Devices of varying loads are using this network, including electric vehicles and large motors. Three-phase transformers with four-wire output are used for 120 volt service. Table 3.1 shows the number of events reported by each power quality meter while the positions of the meters are shown in Fig. 3.2.

The original power quality events reported by our power quality meters carry detailed information where some of the reported attributes are not directly relevant to power quality monitoring. For instance, we have a large number of branch circuit monitors installed that log every 15 minutes. Second, due to the detailed information content, the size of the raw dataset was about 40 GB. In order to simplify the format

Table 3.1: Frequency table showing the number of events generated/reported by each power quality meter.

Meter ID	1	2	3	4	5	6	7	8	9	10
No. of Events	1705	629	756	764	777	282	309	181	44	657

Table 3.2: Frequency table showing the number of events classified as IEEE power quality class (c_i).

	Power Quality Class													
	c_1	c_2	c_3	c_4	c_5	c_6	c_7	c_8	c_9	c_{10}	c_{11}	c_{12}	c_{13}	c_{14}
No. of Events	3056	738	1485	274	144	354	10	11	0	2	8	2	19	1

Table 3.3: Sample events from the dataset collected.

Event ID	**Node ID**	**Duration (seconds)**	**Magnitude (volts)**	**Severity**	**Phase**	**Type**
119	5	0.02	292	3.19	V1	Transient
338	6	1.002	147	47.1	V2	Swell
763	1	0.07	84.4	1.03	V3	Sag

and make the dataset concise and easy to analyze, we transform the reported events into a tabular form consisting of the power quality attributes we used. As a result, there are about 6000 power quality events recorded in the dataset. Sample events from the dataset are shown in Table 3.3.

1. Each row in the table represents a power quality event.

2. The magnitude field represents a percentage of the nominal voltage that the sag or swell reached at its maximum (for instance the number 84 means that voltage is sagged to 84% of its nominal value, 147 means that it swelled up by 47% over its nominal value).

3. The severity field is a calculated statistic that combines the magnitude, duration and class of an event to provide a ranking variable.

Using IEEE Standard 1159 [2], we classify the power quality events based on the fluctuation of the voltage for a predefined period. There are 14 different power quality classes defined in the standard, denoted from c_1 to c_{14}, respectively. Table 3.4 shows samples of the events we classify using the IEEE standard where the power quality class is shown in the last column of the table. The frequency of events belonging to the IEEE power quality class (c_1 to c_{14}) is shown in Table 3.2.

3.4 Capturing the Latent Feature/Transition Function ($f(d)$)

Using the real-world power quality dataset, we capture the device latent feature in three simple steps as follows:

1. **Synchronizing the PQ events:** The power quality meters in our data collection network were configured to report only bad power quality events. We noticed that, in some cases, there are bad power quality events reported at some links while nothing reported by other meters at that time instance. This happens when a device, for instance a UPS, maps a bad quality to good quality. In such cases, we assume a nominal PQ value (PQ class c_{14}) at the monitored but unreported points.

Table 3.4: Sample events classification using IEEE Standard 1159 [2].

Node ID	**Start Time**	**Duration (seconds)**	**Magnitude (volts)**	**IEEE Event Class**
4	733051.9385	0.00065	127	c_1
4	733052.9522	0.00754	146	c_2
8	733452.0117	0.00013	132	c_1
7	733462.7471	0.049	84	c_3
6	733488.8235	1.002	147	c_7
6	733569.0525	0.518	79	c_6
1	733572.9232	0.001	131	c_1
7	733589.9307	0.016	82	c_3
6	733724.0312	7105.48	30	c_{12}
3	733724.1134	0.01664	233	c_4

2. **Building frequency tables:** We now put all the PQ events in a 2-dimensional array $M(i, j)$ of events where the first dimension of the array represents an event i in the time series while the second dimension represents the corresponding event for each device j. We then count the input to output PQ mappings at each device. This results in a 14×14 frequency table ($fr(d)$) for each device d. As an example, frequency table for device d_8 is shown in Table 3.5.

3. **Frequency to probability mapping:** Finally, the transition function is calculated by dividing every element of the frequency table ($fr(d)$) by the sum of the row containing that element, i.e., $f(d, i, j) = fr(d, i, j)/\sum_{k=1}^{14} fr(d, i, k)$. Here, we slightly abuse the notation by using $f(d, i, j)$ to represent the value at the intersection of the i-th row and the j-th column in matrix $f(d)$. Hence, the transition function is represented with a matrix. If every element in a row (say i-th row) of the frequency table is a 0, we assume the same probability (i.e., 1/14) for each element in that row in the transition function, implying that no knowledge can be learned from the dataset about the corresponding input event (c_i) on this device, and as such we assume the maximum uncertainty on its output events to avoid biased estimation. Table 3.6 shows a sample transition function formulated from Table 3.5.

3.5 Cross-validation of $f(d)$

We use k-fold cross-validation technique to measure the accuracy of latent features we learned. We partition the dataset into k random samples of equal size. Out of the k samples, we use $k - 1$ samples to generate a training transition function and one sample to generate the test transition function. The cross-validation is repeated k times where each of the k-samples is used exactly once for validation. The k results are then averaged to produce a single estimation for each device.

The Mean-Square Error (MSE) is used to measure the variation of the validation/test function (represented as $f_v(d)$) from its training function (represented as $f_t(d)$). The MSE is calculated as:

$$mse = \sum_{i=1}^{14} \sum_{j=1}^{14} \mid f_v(d, i, j) - f_t(d, i, j) \mid /(i \times j).$$

Table 3.5: A sample frequency table showing the number of events mapped from input power quality c_i to output power quality c_j at device d_8.

		Output PQ (c_j)					
		c_1	c_2	c_3	c_4	c_6	c_{14}
Input PQ (c_i)	c_3	4	16	4	2	0	113
	c_5	0	0	0	0	0	1
	c_6	0	0	0	0	5	32
	c_7	0	0	0	0	0	2
	c_{12}	1	0	0	0	0	0
	c_{14}	47	48	13	24	2	2122

Table 3.6: A sample transfer function captured at device d_8. Rows and columns having all values set to 0 are omitted.

		Output PQ (c_j)					
		c_1	c_2	c_3	c_4	c_6	c_{14}
Input PQ (c_i)	c_3	0.03	0.12	0.03	0.01	0	0.81
	c_5	0	0	0	0	0	1.00
	c_6	0	0	0	0	0.14	0.86
	c_7	0	0	0	0	0	1.00
	c_{12}	1.00	0	0	0	0	0
	c_{14}	0.02	0.02	0.01	0.01	0	0.94

Table 3.7: Mean Square Errors (MSEs) in estimated and expected probabilities of the transition functions; standard deviation in PQ values of the k-fold test data.

		k-fold cross-validation							
		Mean Square Error				**Standard Deviation**			
		2	10	100	500	2	10	100	500
Device (d_j)	2	0.008	0.012	0.023	0.027	4.37	4.59	4.99	5.04
	3	0.012	0.014	0.028	0.032	4.61	4.51	4.86	5.86
	4	0.014	0.017	0.031	0.036	4.65	4.73	4.82	5.04
	5	0.011	0.013	0.027	0.032	4.71	4.81	5.73	5.77
	6	0.007	0.010	0.021	0.025	2.62	2.89	3.07	4.47
	7	0.024	0.019	0.024	0.026	2.78	3.13	3.43	4.47
	8	0.017	0.015	0.021	0.025	2.38	2.57	3.35	4.59
	9	0	0.002	0.017	0.024	0.89	1.06	1.69	3.89
	10	0.007	0.01	0.021	0.026	3.66	3.72	4.05	5.26

We validate the latent features of all devices on various sample sizes. The largest training sample size is at $k = 2$ where we divide the entire dataset in 2 subsets of equal size; in this case, one subset is used to train the model while the other is used for validation. At the other extreme, at $k = 500$, the dataset is divided into 500 subsets where one of the subsets is used for validation while all other subsets are used for training.

Table 3.7 shows the MSEs for all devices in the network with k-fold cross validation, where k is set to be different values. For each k-fold cross validation test, we also calculated the standard deviation of the k test results. It can be seen that when the value of k increases, the MSEs remain relatively stable with minor changes, but the standard deviation becomes larger. This is reasonable. When k increases, the number of samples in the test dataset becomes smaller, and the transition function built with a small number of samples in the test dataset becomes less accurate and leads to large variance in the test results. Nevertheless, the MSEs together with the standard deviation indicate that the test results with different k values do not exhibit significant statistical differences, and the small MSE values suggest that a device behavior (latent feature) can be captured accurately with historical PQ data from power quality meters.

3.6 Conclusion

In this chapter, we proposed a device latent feature model which learns a device transfer function from real data. The device transfer function is needed to estimate the power quality values on unmonitored links in the power gird. In order to validate the proposed model, We used a real power quality dataset collected by Schneider Electric Inc. in a power grid in Canada. We demonstrated that the historical data can be used to capture the latent features of a device. The k-fold cross-validation technique was used to measure the accuracy of latent features we obtained using our dataset. Experimental evaluations showed that the captured latent features are consistent. The latent features learnt in this chapter are used by our meter placement algorithms proposed in Chapter 6.

Chapter 4

A Data-Driven Network Approach

4.1 Motivation

The power network has many logical and physical similarities with data networks. We model the power network as data-driven network which give us the opportunity to use the well-investigated network monitoring and data estimation algorithms to solve the network quality monitoring in power grids. The proposed network model is described in the next section.

4.2 The Model

We model the power network as a data-driven network, in analogy, where we represent the electrical components as network nodes, power links as data links, and the flow of power as data flow on the links. We assign the power quality on a link at an instance in time as a discrete class (from c_1 to c_n). Aligning with the meters' sampling interval, the time is slotted, and in every time slot, we record a power quality class of each link where a power quality meter is installed.

Moreover, in order to simplify our model, we treat the power flow through each node as a channel (shown in Figure 4.1). The input and output of this channel at each node comprises n power quality classes. The probability that a power quality c_x will be "received" as c_y at the output of the channel at each device d is represented by the symbol $p^{(d)}_{c_y|c_x}$. For each device d, we call the $n \times n$ matrix consisting of the probability values $p^{(d)}_{c_y|c_x}$ the *power quality transition function*, or simply *transition function*. For a device (subnet) having multiple inputs/outputs, a power quality transition function

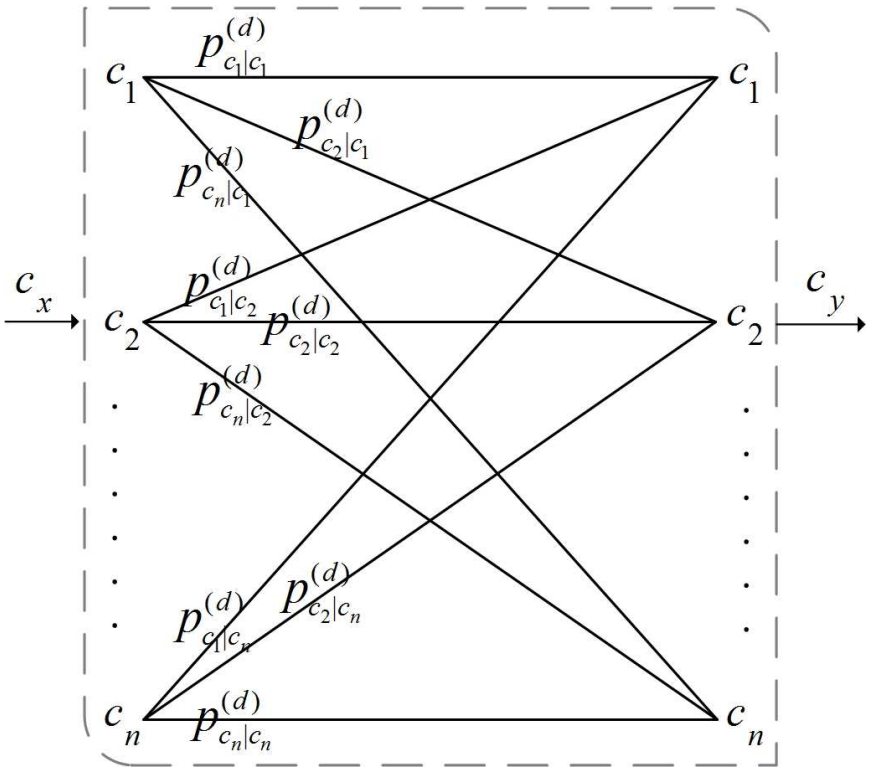

Figure 4.1: Power quality transition at each device d as a channel.

is associated with each input/output pair. We represent the power quality transition function $f(d)$ of a device d as a matrix as

$$f(d) = \begin{bmatrix} p^{(d)}_{c_1|c_1} & p^{(d)}_{c_2|c_1} & \cdots & p^{(d)}_{c_n|c_1} \\ p^{(d)}_{c_1|c_2} & p^{(d)}_{c_2|c_2} & \cdots & p^{(d)}_{c_n|c_2} \\ \vdots & \vdots & \ddots & \vdots \\ p^{(d)}_{c_1|c_n} & p^{(d)}_{c_2|c_n} & \cdots & p^{(d)}_{c_n|c_n} \end{bmatrix}, \tag{4.1}$$

where $p^{(d)}_{c_y|c_x}$ is the probability that the input quality c_x is received as c_y at the output of device d. Note that every row in the above matrix should sum to 1.

The above model significantly simplifies the network complexity of the power grid. Using this analytical model, in the next few chapters, we propose various algorithms for power quality monitoring and demonstrate that this model significantly simplifies our solutions. A short summary of the proposing algorithms as applications of our analytical model is given in the next section.

4.3 Applications

We build various applications on top of the analytical framework we proposed in this Chapter. The applications are as follows.

4.3.1 Power Quality Estimation

Figure 4.2 shows a view of a power grid where there are different types of electrical devices connected to each other via power links. The smart meters are also installed on selected links. Moreover, every type of device has a power quality function which may be unknown. We want to estimate all the power quality functions based on the power quality values available on selected links where smart meters are installed.

In order to estimate the reliability of every device in the network, we need to estimate the power quality function $f(d_j)$ for each device d_j based on the quality function $f(s)$ of the subnet. It is clear that

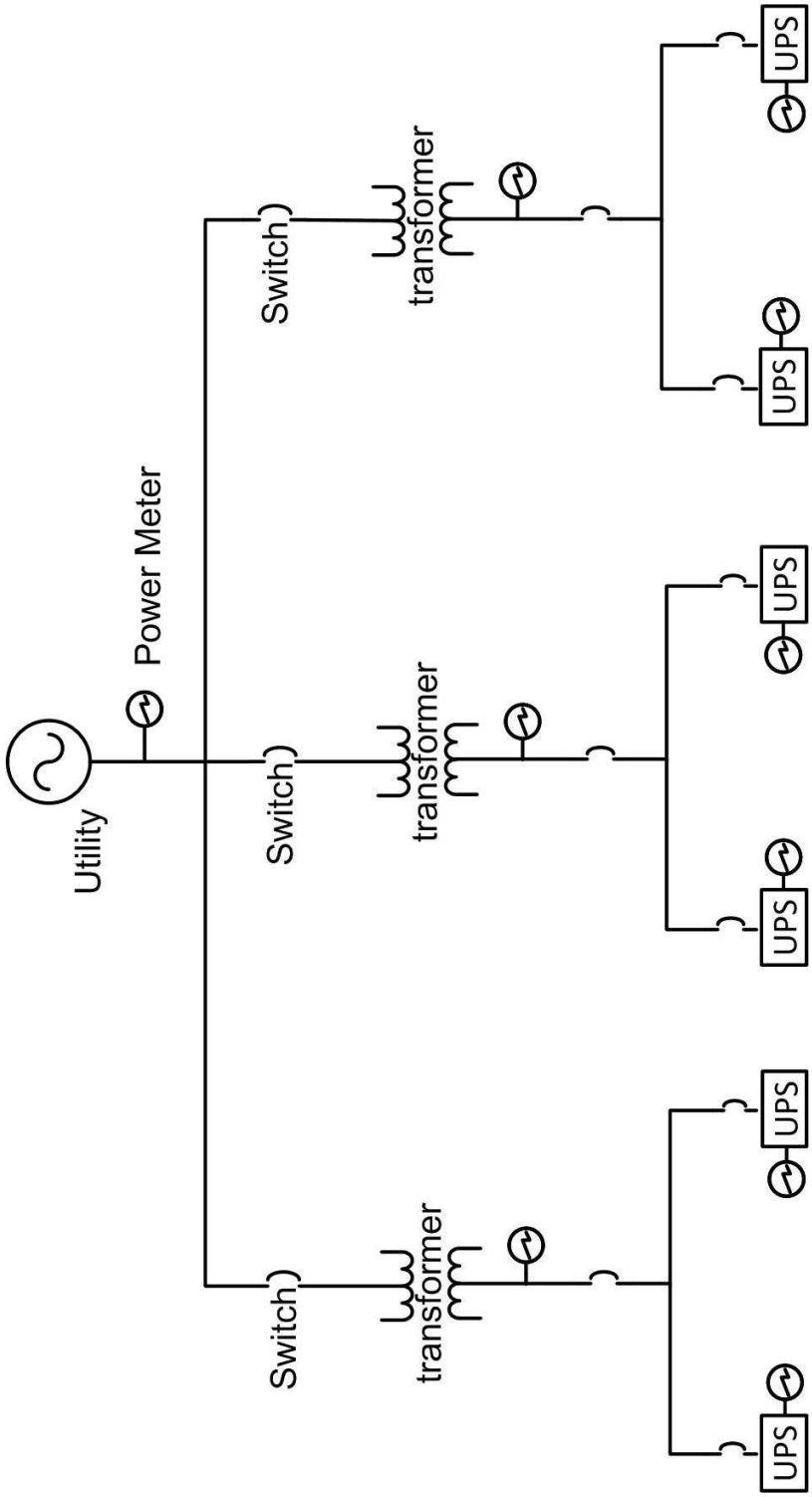

Figure 4.2: A simple view of power microgrid

$$f(s) = \prod_{j} f(d_j), \tag{4.2}$$

Our objective is to estimate $p^{(d_j)}_{c_y|c_x}$ (probability that power quality c_x will be mapped to power quality c_y at each device d_j). In order to solve the above research problem, we model the power network as data network which give us the opportunity to use the already proposed data estimation techniques to solve Eq. (4.2).

4.3.2 Intelligent Meter Placement

For the meter placement problem, we propose an iterative approach for identifying network segments suitable for power meter placement. During each iteration of the algorithm we identify in a greedy manner the network segment that suffers from the most unpredictable power quality given the meters deployed so far. We then deploy the next power meter at that location. Our proposed meter placement algorithms take advantage of our network model to calculate the uncertainty of the power quality values on various network segments.

Similarly, we use the same network model to solve the problem of getting the optimized number of meters required to achieve certain level of reliability. We formulate this problem as an optimization problem where the objective is to reduce the number of meters while maintaining an acceptable level of reliability. In order to calculate the reliability (the uncertainty of power quality) on power links, we use this network model which simplify the representation of the power network as a data network.

4.3.3 Detecting a Malfunction Device

Our third contribution is detecting a malfunction device in the power grid. Since the model we propose to detect a malfunction device uses our meter placement algorithms, the same concept of simplifying the power grid as a data network need to be used here as well. The proposed model is using the exact PQ values from the metered locations and inferred values from the unmetered locations in the network. A device is considered malfunction when it consistently behaving abnormal by generating significantly different PQ values than the expected ones. The acceptable behavior is derived with the help of CBEMA curve.

Chapter 5

Fast Estimation of Power Quality

In this chapter, we propose a maximum-entropy (MaxEnt) based approach to estimating power quality in smart microgrid. Compared to other existing methods such as Monte Carlo Expectation Maximization (MCEM), the MaxEnt based approach is much faster.

5.1 Introduction

Power quality largely impacts the reliability and energy saving of power networks. Poor power quality such as voltage sags may lead to power outage and service interruptions. Service unavailability caused by power losses is a serious problem for many companies and organizations, e.g., it may result in a significant revenue loss for Internet service providers or even loss of lives in hospitals. To improve the reliability of power networks, organizations and large companies (e.g., Google data centers) adopt smart microgrid, and closely monitor the power quality in different segments of the microgrid.

Monitoring power quality, however, is not an easy task. Since the power measurement devices [5][6] (termed as smart meters in this thesis) are expensive, it is financially impractical to monitor every segment of a power network. The overhead of interconnecting these power meters and developing the power management system further increases the cost. In addition, in many cases direct monitoring of power quality is difficult, e.g., it is hard to install smart meters after power lines were sealed in hard-to-reach areas in a building. In general, we need to tackle the following challenge: based on a limited small number of monitored points in a power network, *how can we effectively estimate the power quality of other unmonitored segments of the network?*

We propose to use a Maximum-Entropy (MaxEnt) [7] approach to power quality estimation. The basic idea of MaxEnt is that out of all probability distributions consistent with a given set of constraints (i.e., the known measure values in our case), we should choose the one that has the maximum uncertainty to be the estimated power quality values. Intuitively, the principle of MaxEnt implies that we should make use of all the information that is given and avoid making (biased) assumptions about information that is not available. We model the problem of estimating power quality in such a way where we can effectively get the benefit of MaxEnt approach to correctly estimate the power quality values at links where we do not have any measuring device installed. We solve the formulated MaxEnt problem and validate its effectiveness and efficiency with a simulated microgrid system.

5.2 Related Work

According to the IEEE Gold Book [9], the industry practices for electric power quality in networks focus on measures such as reliability, availability, and Mean Time Between Failures (MTBF). While it is known [8] that lifetime and performance of electrical components are dependent on power quality, none of the measures defined in the IEEE Gold Book accounts for power quality. Moreover, these measures serve as theoretical values for comparisons and are not intended to work in real environment (with varying temperature, humidity, load, and power quality) as predictive tools for networks. Further, the ITI curve report illustrates the relationship between power quality and the likelihood of damage to electric components. While considering the importance of both the magnitude and duration of power quality events in isolation, it does not consider its cumulative effects over time.

The EM algorithm is one of the most widely-used algorithms for estimation and has been applied in a variety of research areas. In [10], the authors investigate the power of EM algorithm in the estimation of microgrid reliability. Although effective, the EM algorithm needs a long time to converge. We are thus motivated to find faster algorithms in power quality estimation for smart microgrid.

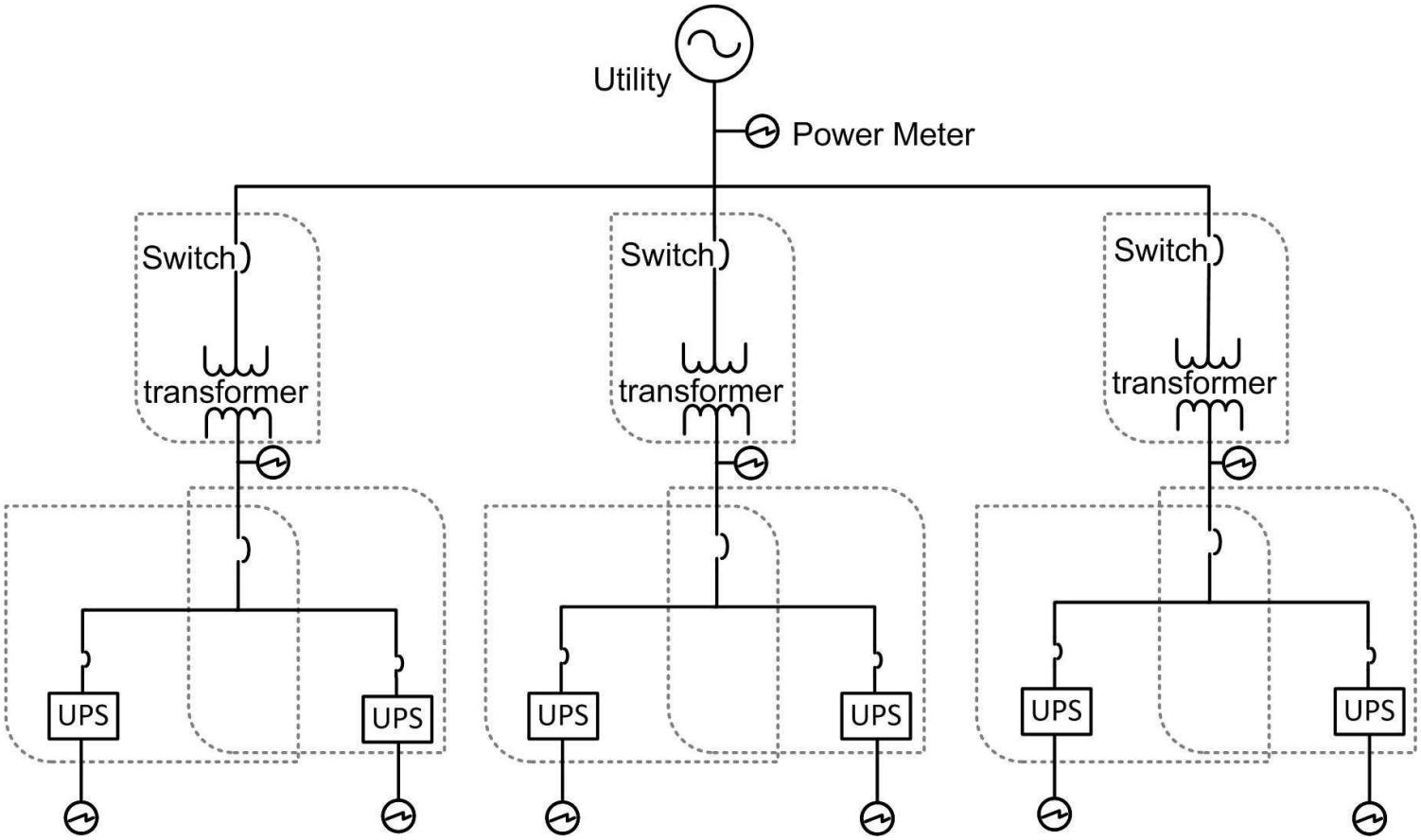

Figure 5.1: View of the power grid network under consideration. Subnets (within dotted lines) are formulated based on the positions of the power meters.

The measurement and monitoring of power quality are a vital part of today's smart grid. To classify power quality, a label is assigned to a power quality event, based on the feature of the event, e.g., the magnitude and duration of a voltage sage or swell. Typically, the power quality index, also known as System Average RMS Variation Frequency Index (SARFI), is reported as a count of the number of times the magnitude and duration fall below a threshold, standardized by the IEEE standard 1159-2009 [2].

5.3 Problem Formulation

Figure 5.1 shows a view of a power grid where there are different types of electrical devices connected to each other via power links. The smart meters are also installed on selected links. Moreover, every type of device has a power quality function which may be unknown. We want to estimate all the power quality functions based on the power quality values available on selected links where smart meters are installed. We divide the power grid network into small subnets where in every subnet we have two smart meters, i.e., one at the input as the first node and one at the output as the last node of the subnet as shown in Figure 5.1.

Now, we consider every subnet as a single node which we call a black-box. For every black-box, we know the power quality values at the input as well as at the output. Based on this known power quality information, we calculate the power quality transition function by using some sample readings from the smart meters attached to both sides of every black-box. Figure 5.2 shows a sample subnet as a single node. We represent the calculated power quality function $f(s)$ of subnet s as a matrix as follows:

$$f(s) = \begin{bmatrix} p^{(s)}_{c_1|c_1} & p^{(s)}_{c_2|c_1} & \cdots & p^{(s)}_{c_n|c_1} \\ p^{(s)}_{c_1|c_2} & p^{(s)}_{c_2|c_2} & \cdots & p^{(s)}_{c_n|c_2} \\ \vdots & \vdots & \ddots & \vdots \\ p^{(s)}_{c_1|c_n} & p^{(s)}_{c_2|c_n} & \cdots & p^{(s)}_{c_n|c_n} \end{bmatrix}, \tag{5.1}$$

where $p^{(s)}_{c_y|c_x}$ is the probability that the input quality c_x is received as c_y at the output of the subnet s. Moreover, the value of $p^{(s)}_{c_y|c_x}$ can be easily calculated by measuring power quality values at the input and output smart meters of the subnet. Note that every row in the above matrix must sum to 1.

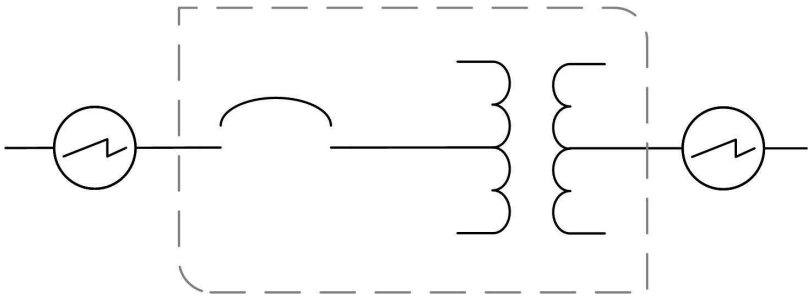

(a) A subnet containing 2 devices.

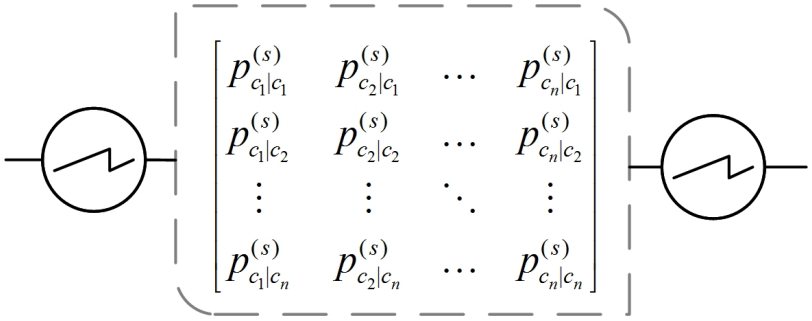

(b) Subnet as a single power transition matrix.

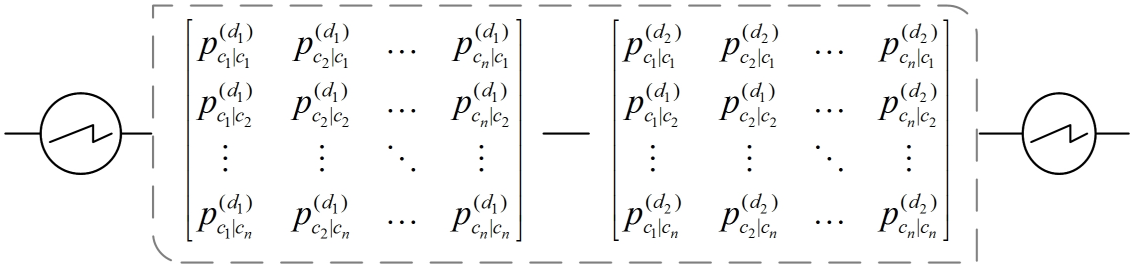

(c) Power transition matrix of each device d_j.

Figure 5.2: Subnet power transition matrix as a product of power transition matrices of individual devices.

Figure 5.2(a) shows a subnet containing two devices. The power quality transition function (as a matrix) of the subnet is shown inside the black-box in Figure 5.2(b). Our objective is to correctly estimate the transition functions of every device d_j in the subnet. These unknown functions are shown as matrices in Figure 5.2(c).

In order to estimate the reliability of every device in the network, we need to estimate the power quality function $f(d_j)$ for each device d_j based on the quality function $f(s)$ of the subnet. It is clear that

$$f(s) = \prod_j f(d_j), \tag{5.2}$$

which implies that

$$\begin{bmatrix} p^{(s)}_{c_1|c_1} & \cdots & p^{(s)}_{c_n|c_1} \\ \vdots & \ddots & \vdots \\ p^{(s)}_{c_1|c_n} & \cdots & p^{(s)}_{c_n|c_n} \end{bmatrix} = \prod_j \begin{bmatrix} p^{(d_j)}_{c_1|c_1} & \cdots & p^{(d_j)}_{c_n|c_1} \\ \vdots & \ddots & \vdots \\ p^{(d_j)}_{c_1|c_n} & \cdots & p^{(d_j)}_{c_n|c_n} \end{bmatrix} \tag{5.3}$$

Our objective is to estimate $p^{(d_j)}_{c_y|c_x}$ (probability that power quality c_x will be mapped to power quality c_y at each device d_j). We use the data estimation techniques to solve Eq. (5.3).

5.4 Power Quality Estimation using Entropy Maximization

Modeling the microgrids as data-driven networks helps us utilize the best available data estimation techniques to solve the power quality estimation problem. One of the most popular and widely-used data estimation techniques is EM algorithm. In a recent study [10], the authors successfully applied the EM algorithm to power quality estimation in microgrid. Although effective, the EM algorithm took a long time to converge. In this work, we propose to use a MaxEnt approach to estimating the power quality of unmonitored segments of the grid. Before we formulate the power quality estimation problem as a MaxEnt problem, first we give a short description of EM and MaxEnt algorithms:

- **The Expectation Maximization (EM):** EM is a general approach to iterative computation of maximum-likelihood estimates when the observations

can be viewed as incomplete data. Since each of the iteration of the algorithm consists of an expectation step followed by a maximization step, the algorithm is named as the EM algorithm. The successive iterations always increase the likelihood and the algorithm converges at a stationary point.

- **MaxEnt:** MaxEnt solves convex optimization problems of the form,

$$\textbf{maximize } g(\vec{x}) = -\sum_{i=1}^{n} x_i \log x_i$$

$$\text{subject to } \mathbf{A}\vec{x} \leq \mathbf{c},\ \mathbf{B}\vec{x} = \mathbf{1},$$

where $\vec{x} \in \mathbb{R}^n$ is the optimization variable, $A \in \mathbb{R}^{m \times n}$, and $B \in \mathbb{R}^{m \times n}$ are problem parameters; and $\mathbf{1}$ is a vector with all 1's.

Now, we model the power quality estimation problem as the MaxEnt problem to accurately estimate the power quality transition functions $f(d_j)$ with acceptable efficiency. Obviously, there are multiple possible power quality functions $f(d_j)$ which are consistent with Eq. (5.3). We consider only those solutions which not only satisfy Eq. (5.3) but are consistent with other design constraints, for instance: 1) every row in the matrix $f(d_j)$ must sum to 1 (or at least very close to 1); and 2) $p^{(d_j)}_{c_y|c_x}$ must not be negative. Other possible constraints are discussed later in this section.

The basic idea of using MaxEnt here is that out of all possible quality functions (probability distributions) consistent with the design constraints, we choose the one with maximum uncertainty. Intuitively, the principle of MaxEnt implies that we should make use of all the information (design constraints) that is available and avoid making (biased) assumptions about information that is not available. Our objective function becomes,

$$\textbf{maximize } g = -\sum_{j,\ x,\ y} p^{(d_j)}_{c_y|c_x} \log p^{(d_j)}_{c_y|c_x} \tag{5.4}$$

subject to following constraints:

1. All components of the estimated functions $f(d_j)$ must not be negative, that is,

$$p^{(d_j)}_{c_y|c_x} \geq 0 \tag{5.5}$$

2. Every row of $f(d_j)$ sum to 1. To allow negligible rounding errors, we introduce

a small rounding error factor (ε_1) to be tolerated, i.e.,

$$\left| 1 - \sum_{y} p^{(d_j)}_{c_y|c_x} \right| \leq \varepsilon_1, \quad \forall x \tag{5.6}$$

3. The estimated functions $f(d_j)$ satisfy the condition $\prod_j f(d_j) = f(s)$. One may relax the condition by a small approximation error factor (ε_2) to adjust the rounding errors. This adjustment is necessary when we are interested in a close approximation of $f(s)$. This condition becomes,

$$\left| f(s) - \prod_{j} f(d_j) \right| \leq \varepsilon_2. \tag{5.7}$$

   Note that we slightly abuse the notation for simplicity. We use $-$ above to represent an element wise minus of two matrices and $|.|$ to change the values in the matrix to their absolute values. In addition, the symbol $\leq$ means all values in the left matrix is no larger than ε_2.

4. Every component of the estimated function $f(d_j)$ must not vary from its corresponding component of the "true" transition function $\acute{f}(d_j)$ by a factor ε_3, i.e.,

$$\left| f(d_j) - \acute{f}(d_j) \right| \leq \varepsilon_3 \tag{5.8}$$

   The meanings of the notations are the same as above.

Remark 1. *In practice, we do not know $\acute{f}(d_j)$. To avoid this problem, we can initially set $\acute{f}(d_j)$ as the transition function of the same type of device, which may be obtained via its specification or historical data of monitored devices of the same type. As time goes, this initial setting of $\acute{f}(d_j)$ should be updated with the optimal estimation function, i.e., $\acute{f}(d_j)$ is set to equal $f(d_j)$, and the updated $\acute{f}(d_j)$ is used for the next round of estimation. Such iterative updates capture the transition function of the (unmonitored) device, which may change over time.*

Remark 2. *Someone may argue that our solution may be biased toward the last constraint (i.e., Eq. 5.8). By ignoring the last constraint, we get many solutions consistent to the first three constraints and our objective function chooses the one having maximum uncertainty. Here, if we do not use constraint 4 (Eq. 5.8), we will*

be ignoring some known information about the transition functions of the unmonitored devices which may result in compromising the accuracy of the estimated transition functions. Further, in some rare cases, the last constraint may not be feasible when an obtained transition functions ($f(d_j)$) is different by an amount greater than ε_3 . In that case, we may ignore the last constraint or increase the value of ε_3.

Remark 3. *It is worth noting that the objective function (5.4) is a non-Shannon measure, because $\sum_{j,\ x,\ y} p^{(d_j)}_{c_y|c_x} = \sum_j \sum_x \sum_y p^{(d_j)}_{c_y|c_x} > 1$. Nevertheless, by maximizing this non-Shannon measure, we obtain a good estimation of transition functions as demonstrated in our experimental evaluation. This is not by coincidence, since the objective function could be considered as the sum of several Shannon entropy functions (i.e., Given x and j, $\sum_y p^{(d_j)}_{c_y|c_x} \log p^{(d_j)}_{c_y|c_x}$ is a Shannon entropy measure). In our case, we treat each entropy function with the same weight. If we have more knowledge regarding the distribution of input power quality events, assigning different weights to different entropy functions may lead to better estimation. We leave this exploration as future work.*

Remark 4. *This work focuses on a centralized processing and as such we assume that there exists an underlying communication system to support data collection to a central point. The implementation of this communication system is beyond the scope of this work. Further, the real-time issues of the monitoring and communication systems such as the data sampling and communication delay are ignored in the work.*

5.5 Performance Evaluation

We implement the proposed objective function and simulate a power microgrid using MATLAB. The view of the simulated network is shown in Figure 4.2 where only several network segments are monitored using smart meters. Our objective is to estimate the power quality values on network segment where no smart meter is installed. We use the same transition functions as in [10] as the ground truth. These power quality transition functions of various electrical components (switch, bus, ups, and transformer etc) in the smart grid are shown in Table 5.1.

We use non-linear constrained optimization algorithm named Sequential Quadratic Programming (SQP) to estimate the unknown power quality functions. Inputs to the algorithm are the known power quality functions for each subnet $f(s)$, error tolerance factors $\varepsilon_1 = \varepsilon_2 = 0.01$, and $\varepsilon_3 = 0.05$. The error tolerance is small enough

Table 5.1: Transition Functions of Various Electrical Components Obtained Using Our Latent Feature Model

		Output PQ				
		c_1	c_2	c_3	c_4	c_5
Input PQ	c_1	0.9	0.1	0	0	0
	c_2	0	0.9	0.1	0	0
	c_3	0	0	0.9	0.1	0
	c_4	0	0	0	0.9	0.1
	c_5	0	0	0	0	1

(a) Bus

		Output PQ				
		c_1	c_2	c_3	c_4	c_5
Input PQ	c_1	0.7	0.1	0.1	0.05	0.05
	c_2	0	0.7	0.1	0.1	0.1
	c_3	0	0	0.7	0.2	0.1
	c_4	0	0	0	0.7	0.3
	c_5	0	0	0	0	1

(b) Switch

		Output PQ				
		c_1	c_2	c_3	c_4	c_5
Input PQ	c_1	0.85	0.15	0	0	0
	c_2	0.15	0.7	0.15	0	0
	c_3	0	0.15	0.7	0.15	0
	c_4	0	0	0.15	0.7	0.15
	c_5	0	0	0	0	1

(c) Transformer

		Output PQ				
		c_1	c_2	c_3	c_4	c_5
Input PQ	c_1	1	0	0	0	0
	c_2	0.8	0.2	0	0	0
	c_3	0.8	0	0.2	0	0
	c_4	0.8	0	0	0.2	0
	c_5	0.8	0	0	0	0.2

(d) UPS

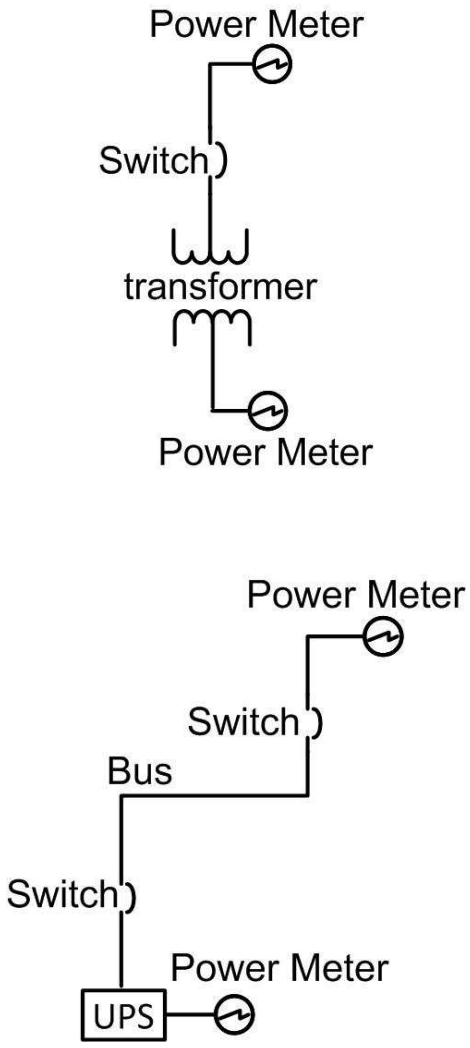

Figure 5.3: Two different kinds of subnets. The one at the left side containing two devices (switch, transformer) and the one shown at the right side containing four devices (switch, bus, switch, and UPS).

Table 5.2: Convergence time (in seconds) comparison of MaxEnt vs EM algorithms.

		MaxEnt	**Expectation Maximization (EM)**		
			Iteration 5	Iteration 10	Iteration 15
Subnet size	2	2.16	40.3	117.7	402.6
	4	3.42	118.32	366.9	981.01

Table 5.3: Mean Squared Error comparison of MaxEnt vs EM algorithms.

		MaxEnt	**Expectation Maximization (EM)**		
			Iteration 5	Iteration 10	Iteration 15
Subnet size	2	0.00020	0.00017	0.00013	0.00010
	4	0.00030	0.00025	0.00019	0.00014

for practical applications. The power quality matrix of each subnet is the product of the power transition functions (shown in Table 5.1) of the devices in that subnet. The simulated microgrid consists of subnets of two different sizes; one contain two devices (switch and a transformer) while the other containing four devices (switch, bus, switch, and UPS). Both of these subnets are shown in Figure 5.3. The power transition matrices of each subnet are calculated by multiplying the ground truth matrices of devices used in the corresponding subnet. Further, the simulation was performed on a desktop computer having Intel Dual-Core-i7 3.4 GHz processor with 4 GB physical memory.

Table 5.2 shows the convergence time comparison of both the EM and MaxEnt based solutions to power quality estimation. It can be seen that the convergence time of MaxEnt is much faster as compared to that of EM algorithm. We measure the estimation accuracy using Mean Squared Error (MSE), which is a statistical measure quantifying the difference between values implied by an estimator and the true values of the quantity being estimated. The results are shown in Table 5.3. From the results, we can see that both the methods give very close estimations of the power quality transition functions, i.e., the difference between the estimated and corresponding ground truth functions is negligible.

5.6 Conclusion

Reliability of power grid networks is critically important in today's life. Smart meters play an important role in estimating reliability of power networks but they are expensive devices and it is financially infeasible to install them on every link between devices in the power grid network. We propose a MaxEnt based model that accurately estimates power quality transition functions on unmonitored network segments. The experimental results show that 1) our MaxEnt based solution is much faster than the existing EM based solution to power quality estimation; and 2) the proposed solution accurately estimates the power transition functions. Finally, the MaxEnt based model opens a new scope of methods to quantitatively measure and solve the reliability problems in smart grid.

Chapter 6

Intelligent Meter Placement

In this chapter, we solve the meter placement problem using entropy-based measurements and Bayesian network models to identify the most suitable power links for power meter placement. To ease understanding, we list the nomenclature used in this chapter first.

Nomenclature

$f(d)$	Device transfer function for a device d
$c_i^{(d)}$	Power quality of class i at device d
C_i	Set of $c_i^{(d)}$ $\forall$ d
$p_{c_y \mid c_x}^{(d)}$	Probability that c_x will be mapped to c_y at device d
$\widehat{d}$	Parent node of a node d
$\breve{d}$	Child node of a node d
d_i	Inferred device
d_o	Observed device
F	Conditional transfer function of device d_o given d_i
$l_{out}^{(d)}$	Output link of device d
$l_{in}^{(d)}$	Input link of device d

6.1 Introduction / Motivation

Monitoring power quality is not an easy task. Since the power quality measurement devices [6] are expensive, it is financially impractical to monitor every segment of a

power network. The overhead of interconnecting these power meters and developing the power management system further increases the cost. Therefore, we need to intelligently place power quality meters on selected power links to reduce the uncertainty of power quality estimation on unmonitored links in the power grid. The following core challenge needs to address: given a fixed number of available power meters, which grid segments should be selected for monitoring such that power quality can be inferred in the remaining unmonitored segments of the network.

As the first step to tackle the above challenge, the probabilistic calculation of power quality values on unmonitored links requires the behavior (latent feature) of each device to be known. We represent the latent feature of a device as a transition function which is usually estimated through physical modeling or through the assessment of historical power monitoring data. Using a real power quality dataset, we show that historical data can be used to capture the latent features of a device.

With devices' latent features captured, we in the second step introduce a network model which represents the smart microgrid as a data-driven network. In analogy, we represent the electrical components as network nodes, power links as data links, and flow of power as data flow on the links. This problem transformation significantly simplifies the complexity of the power network; it also presents the opportunity to use the well-investigated network monitoring and data estimation algorithms to solve the network quality monitoring problem.

Finally, we solve the intelligent meter placement problem by proposing an iterative approach for identifying network segments suitable for power meter placement. During each iteration of the algorithm we identify in a greedy manner the network segment whose power quality is most unpredictable given the meters placed so far. We then place the next power meter at that location. In this chapter, we make the following contributions.

1. A network model for power quality estimation, based on the device latent features that are learned from a real-world dataset,

2. An intelligent entropy-based algorithm and a Bayesian network based approach to solve the meter placement problem.

3. Formulate the problem of estimating the number of required power meters to achieve the desired level of reliability as an optimization problem.

6.2 Related Work

This work is related to four categories of research and development: power quality (PQ) classification, power reliability, power quality improvement/estimation, and meter placement. We summarize the relevant literature in these categorize in Section 2.3. We re-iterate the three main differences between the existing PMU placement algorithms and our proposed algorithm as follows.

1. We focus on distribution networks at the enterprise level (e.g., a university campus).

2. Our method is data driven and is based on statistical machine learning method.

3. The existing PMU placement algorithms address the problem of estimating network states and do not consider power quality estimation explicitly.

6.3 Meter Placement Problem Formulation

Before we formally illustrate our proposed algorithms for the deployment of power meters in the electric power grid, we detail our assumptions about the structure and function of the power grid network as follows:

1. *The power grid network is a tree-structured network where the electric current flows from root node to the child nodes.* Note that this is a reasonable assumption at any particular instance in time. While enterprise level power grids used in places such as hospitals and data centers often have two utility feeds available as well as an independent emergency power source, only one power source is typically used at one time. See the IEEE Gold Book [9] for further information on recommended practices in the design of critical power systems.

2. *The probability mass function (pmf) of power quality values at the input link to the root node is known.* In other words, the distribution of power quality at the input to the network, usually the utility feed, is known. This is also a reasonable assumption, since electrical utilities typically report on indices such as System Average RMS Variation Frequency Index (SARFI) which is essentially a count of the number of times the magnitude and duration falls below a threshold. Furthermore, there are often independent bodies that gather

statistics on power delivery service reliability that can also be incorporated into an estimate of power quality distribution [24].

3. *The power quality transfer function $f(d)$ is known for every device d.* A device-specific power quality transfer function could be estimated for specific models of electrical components through physical modeling or through the assessment of historical power monitoring data. Given a reasonable initial estimate, the transfer functions could be further refined through online learning techniques [10].

Given the assumptions listed above we can define a power meter placement algorithm as a process that takes as an input: the topology of the smart grid, an *a priori* estimate of the feed *pmf*, the power quality transfer function for each component, and the total number of meters M. The output of the algorithm is a set of L locations for deploying power meters.

6.4 Meter Placement Algorithms

6.4.1 A Simple Entropy-Based Approach

We propose to deployed the power quality meters on network segments where the power quality values are most uncertain. We measure the uncertainty of power quality on a link using Shannon's entropy measure. Therefore, the entropy formula to measure uncertainty at the output link of a device d becomes

$$H(d) = H(l_o^{(d)}) = -\sum_{i=1}^{n} p_{c_i}^{(d)} \log p_{c_i}^{(d)},$$

where $p_{c_i}^{(d)}$ is the probability of power quality c_i at the output link of device d.

In order to calculate $H(d)$, we need to know the power quality distribution function of link $l_o^{(d)}$. Starting from the root node of the tree-structured network, we traverse all the nodes (devices) in level-order fashion to calculate the distribution function $f_x(d)$ as $f_x(d) = f_x(\hat{d}) \times f(d)$. After calculating $f_x(d) = [p_{c_1}^{(d)}\ p_{c_2}^{(d)}\ \ldots\ p_{c_n}^{(d)}]$ where $p_y(d) = \sum_{x=1}^{n} p_x^{(d)} \times p_{c_y|c_x}^{(d)}\ \forall\ y = 1, 2, \ldots, n$.

The detail of our entropy-based meter placement algorithm is shown as Algorithm 1 where the power meters are placed on network segments having maximum uncertainty in power quality values. This simple algorithm is fast and useful when

Algorithm 1: A Simple Entropy-Based Algorithm

Input: distribution function of input link to device 1 i.e., $f_x^{(0)}$, transfer function $f(d)$, and number of power meters M.

Output: L (list of devices to be selected for meter placement)

begin

  foreach *(device d)* **do**

    $\hat{d} \leftarrow getParent(d)$;

    /* Note that device 1 (root of the tree) has no parent i.e., *getParent(1) = 0* and $f_x(0)$ is given */

    $f_x(d) \leftarrow f_x(\hat{d}) \times f(d)$;

    $H(d) \leftarrow -\sum_{i=1}^{n} p_{c_i}^{(d)} \log p_{c_i}^{(d)}$;

    /* where $p_{c_i}^{(d)}$ is the i^{th} component of $f_x(d)$ vector */

  end

  /* get N high entropy devices in vector H */

  $L \leftarrow getHighEntopyDevices(H, N)$;

end

there is negligible impact of a link on any other link in the network. For instance, if a node always produces a power quality c_1 as output irrespective of the input quality (a stabilizer). Nevertheless, in most cases the network links are dependent on each other. Therefore, we need to consider the link dependency while calculating the uncertainty of a link, i.e., a meter reduces the entropy not only on the measured link, but also on other links in the network. Further, based on our initial tests with the simple Algorithm 1, we conclude that it may create a poor allocation scheme for some cases. In the remainder of this section, we further investigate the problem and propose more robust methods to address the power meter placement problem.

6.4.2 Bayesian Network Based Approach

This section describes a Bayesian network based algorithm for selecting locations for placing power meters in a power grid. The approach uses Monte Carlo sampling and probabilistic inference approaches to identify locations in the power grid which exhibit unpredictable power quality events.

The problem is inherently challenging as the information received from a power meter flows not only the forward direction from the root nodes toward the leaf nodes, but also in reverse or upstream direction toward the root node (utility main) and back to all other nodes in the network.

To tackle the above challenge, we cast the problem as a Bayesian network and model the power grid using a factor graph. Several message passing algorithms could be used to help us determine the optimal meter placement. We chose the belief propagation or sum-product algorithm [22], since it is well understood and has been shown to work for general topologies [23] including tree networks.

MC Event Sampling

Given the transition function $f(d)$, we use a Monte Carlo (MC) method to obtain a set of K samples at each node d. We first compute a *pmf* $f_x(d)$ for each node d using its transition function $f(d)$ and the *pmf* of its parent node $\widehat{d}$ as $f_x(d) = f(d) \times f_x(\widehat{d})$. Then, at each time slot $i \in \{1 \dots K\}$, we draw a sample $c_i^{(d)}$ from $f_x(d)$ at each node d. We repeat this at each node of the tree starting from the root and ending at the leaves. The result is a set of K simulated samples $C_i = \{c_i^{(1)}, c_i^{(2)}, \dots, c_i^{(N)}\}$ for each of the N links in the power network.

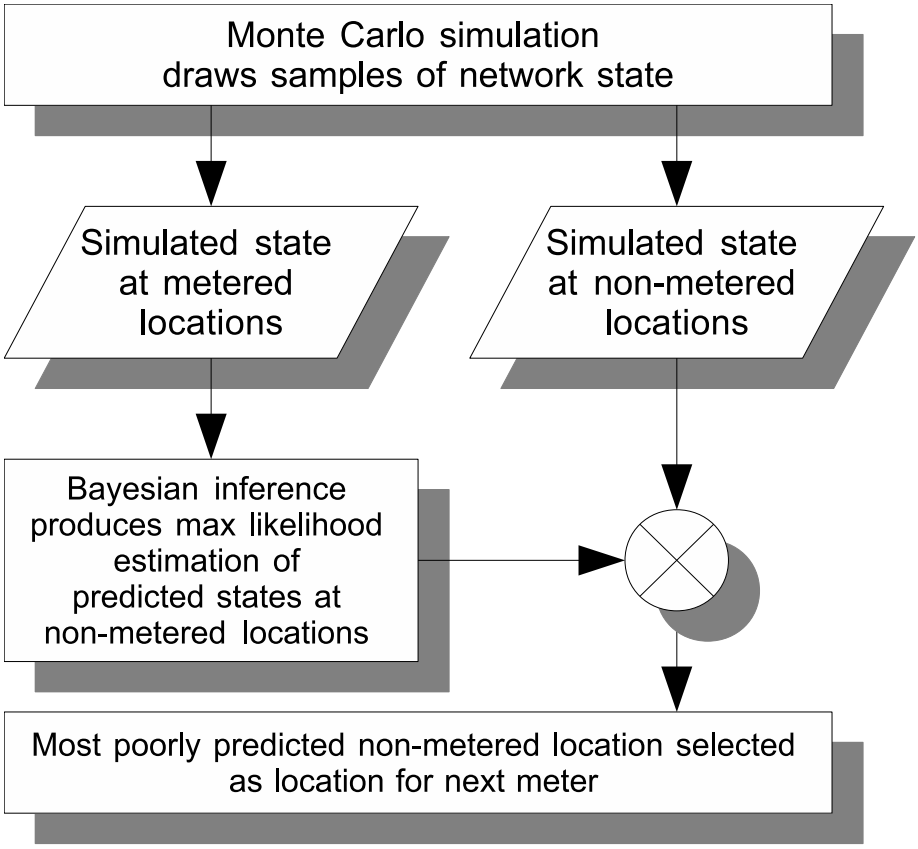

Figure 6.1: Data flow diagram of meter selection process during a single iteration of the greedy algorithm.

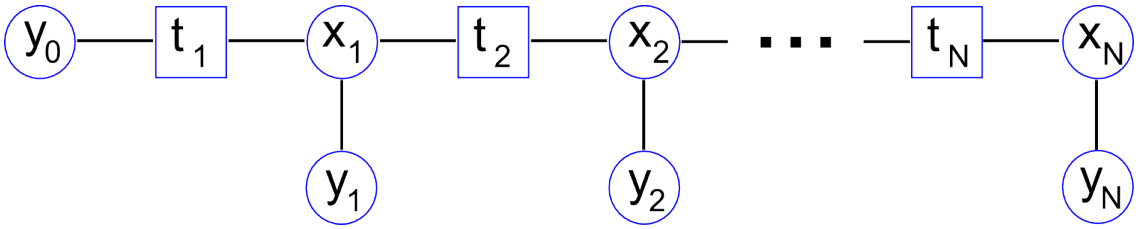

Figure 6.2: Power network modeled as a factor graph

Event Inference using Belief Propagation

The samples obtained by the MC simulation of power quality propagation contain consistent sets of power quality values at both metered and unmetered locations. We use Bayesian inference to infer the power quality at unmetered locations as a function of the simulated values observed at the metered locations and compare the resulting predictions to the simulated value seen at the unmetered locations. This process gives a relative indication of the predictive strength on each link of the network. Figure 6.1 shows a high-level description of this process.

To do the prediction, we first model the power network as a factor graph (Figure 6.2) and then use belief propagation to find the inferred values of power quality at the output of each node using the (simulated) evidence obtained from the power meters. The factor graph has conditional probability nodes t, equality nodes x, and evidence nodes y. The t nodes represent actual electrical devices with a known transition function. The x nodes represent wired connections on our network for which we have already obtained a set of samples using MC sampling. These nodes are constrained so that all edges connected to them are equal. The y nodes represent locations where a power meter could be placed. The unmetered nodes are initialized to a uniform *pmf* and the metered nodes are set to a trivial *pmf* with a probability of 1 at the true power quality event and 0 everywhere else.

For each time slot t_i we infer the maximum likelihood power quality event that would appear at each node given the current meter configuration. We then estimate the error rate for each node in the network. If the inferred event differs from the event given by the MC sample we add $1/K$ for that sample. At each round of the algorithm we greedily choose to place a meter at the node with the highest error rate. We terminate the algorithm when all meters have been placed.

The number of required power quality meters could be determined based on: 1) the available financial budget, and 2) the desired estimation accuracy. We consider both aspects. The proposed algorithms keep placing meters until either the maximum meter limit is exhausted or the desired estimation accuracy is achieved. The estimation accuracy is captured by the certainty of PQ values on network segments. See Algorithm 2 and Figure 6.1 for further details.

Algorithm 2: Monte Carlo Predicted Error Algorithm

Input: The topology T of the power grid, the input feed to first device $f_x(0)$, transition functions $f(d)$, maximum number of meters M_{max}, maximum uncertainty to allow δ_{max}, and the number of Monte Carlo samples K to draw.

Output: L (list of links to be selected for meter placement)

begin

$M \leftarrow 0$; $\delta_{curr} \leftarrow \delta_{max}$;

while *($M < M_{max}$ and $\delta_{curr} \geq \delta_{max}$)* **do**

$\epsilon_l \leftarrow 0, \forall$ links $l \in T$;

/* ϵ_l is prediction error at link l */

foreach *(Monte Carlo Sample k)* **do**

$L \leftarrow$ set of metered links $\in T$;

$L' \leftarrow$ set of unmetered links $\in T$;

$\widehat{C}_k \leftarrow$ predictPowerQuality(L', L, T);

/* $\widehat{C}_k$ is the k^{th} set of predicted power quality values while C_k is the k^{th} set of sampled values at all links*/

foreach *(link $l \in L'$)* **do**

if $\widehat{c}_k^{(l)} \neq c_k^{(l)}$ **then**

$\epsilon_l \leftarrow \epsilon_l + \frac{1}{K}$; /* add $\frac{1}{K}$ to predicted error */

end

end

end

$selectedLink \leftarrow \max(\mathcal{E}).position$;

/* $\mathcal{E} = \{\epsilon_l\}$ i.e., set of $\epsilon_l \; \forall \; l$ */

L.add($selectedLink$);

$\delta_{curr} \leftarrow \max(\mathcal{E})$; $M \leftarrow M + 1$;

end

end

function predictPowerQuality$(L', L, T) : C_k$

begin

init pmf $\Psi = \{\psi_l\}, \forall$ links $l \in T$;

$\Psi' \leftarrow$ BeliefPropogation given evidence L

foreach *(link $l \in L'$)* **do**

$c_k^{(l)} \leftarrow$ max probability power quality class inferred in ψ'_l;

end

$C_k = \{c_k^{(l)}\}$;

end

6.4.3 Conditional Entropy (CE) Based Approach

Since the PQ values on network segments are dependent on each other, we exploit the idea of conditional entropy to propose another new algorithm. Further, this approach is much faster than the Bayesian network (BN) based approach without compromising the accuracy. The idea here is to install each power meter under consideration on a network segment i which results in maximum reduction in overall network entropy. We consider all possible placement points for every meter to be placed and choose a link which reduce the network entropy at maximum. Note that a reduction in network entropy is the sum of entropy reduction on the underlying link i and all other links whose entropy is minimized/reduced in effect of meter placement on a segment i. The one time matrix multiplications in this approach are much faster than our previous requirement of re-sampling the network state after every possible meter placement.

The CE based algorithm is efficient and scalable to large scale real-world networks. Both the BN and CE approaches are based on similar concepts of predicting the state of PQ values at unmonitored links given the current network configuration (positions of meters already placed). The CE based approach, which we will call MinEntropy, uses a heuristic to combine evidence but results in orders of magnitude faster running time.

Methodology

As discussed earlier in this paper, the uncertainty of power quality values on a link is dependent on the uncertainty of power quality values on other links (parents, children, sibling nodes etc) in the network. Therefore, any new information about PQ values at a link increase our belief of the PQ values on other dependent links in the same network. Technically, the entropy of any link in the network is reduced by an amount of ≥ 0 by knowing the values of PQ on any other link in the network. We also know that, the entropy of a link given another link is always less than or equal to its original entropy i.e., $H(Y \mid X) \leq H(Y)$. Since every link $l_{out}^{(d)}$, if chosen for meter placement, influences the uncertainty of PQ values on other links, we consider the conditional entropy of all monitored links while placing power meter at a link $l_{out}^{(d)}$.

Now, the conditional entropy of a link $l_{out}^{(d_i)}$ (the output link of the inferred device d_i) given the meter is being installed on a link $l_{out}^{(d_o)}$ (the output link of the device d_o)

is calculated using the formula

$$H(Y \mid X) = \sum_{x \in X} \left(p(x) \sum_{y \in Y} p(y \mid x) \log(\frac{1}{p(y \mid x)}) \right),$$

where X and Y are the distribution functions of the output links of d_o and d_i respectively. We write the above equation in terms of our power quality distribution vector $f_x(d_o)$, device transition matrix $f(d_i \mid d_o)$ as:

$$H(Y \mid X) = -\sum \Big(f_x(d_o) \times \big(F \otimes \log f(d_i) \big) \Big),$$

where $\times$ represents the cross product, the symbol $\otimes$ represents the dot or component-wise product (also known as Hadamard product), and log is a component-wise log operation. Further, the $\sum$ operation is the summation of components of the resulting vector after $\otimes$ and then $\times$ operations, and F is the conditional transition function representing $f(d_i \mid d_o)$. Depending on the positions of d_o and d_i, F is calculated in one of the three methods as follows:

1. **Observed device d_o is a parent of d_i**: Here, the conditional transition function $f(child \mid parent)$ is simply the product of the normal transition functions of devices between links $l_{out}^{(d_o)}$ and $l_{out}^{(d_i)}$, i.e.,

$$F = f(\breve{d_o}) \times \ldots \times f(d_i).$$

2. **Observed device d_o is a child of d_i**: We calculate the influence of a child device on a parent device. Note that the parent may not necessarily be the immediate parent. To calculate the entropy of parent given child using the general formula of conditional entropy, we need to first calculate the conditional transition function F.

   We use the concept of posterior probability (the Bayes theorem) to calculate F. This function is simply the product of the reverse transition functions of devices all the way from child to parent. The reverse transition function $f'(d)$ (consist of $p(parent \mid child)$ or $p(X \mid Y)$) is calculated as $p(X \mid Y) = \frac{p(X)p(Y/X)}{p(Y)}$. In our case, the function $f'(d)$ of a device d which list $p(x \mid y)$ in the xth row and yth

column is calculated as:

$$f'(d) = \begin{bmatrix} f_x(\widehat{d}) \\ f_x(\widehat{d}) \\ \vdots \\ f_x(\widehat{d}) \end{bmatrix} \otimes \big[f(d)\big]^T \oslash \begin{bmatrix} f_x(d) \\ f_x(d) \\ \vdots \\ f_x(d) \end{bmatrix}^T,$$

where $\otimes$ is the component-wise product, $\oslash$ is the component-wise division, and $\widehat{d}$ is the immediate parent of device d. Finally:

$$F = f'(d_o) \times f'(\widehat{d_o}) \times \ldots \times f'(\breve{d}_i).$$

3. **Devices d_o, d_i belong to different sub-trees**: This is an interesting case where the devices d_o and d_i belong to two different sub-trees rooted by a device d_r. In this case, F is calculated in two steps. First, we calculate the conditional transition function $f(d_r \mid d_o)$ of devices between links $l_{out}^{(d_o)}$ and $l_{out}^{(d_r)}$ using method 2. We then calculate the conditional transition function $f(d_i \mid d_r)$ of devices between links $l_{out}^{(d_r)}$ and $l_{out}^{(d_i)}$ using method 1. Finally:

$$F = f(d_i \mid d_o) = f(d_r \mid d_o) \times f(d_i \mid d_r)$$

The MinEntropy Algorithm

Algorithm 3 illustrates our conditional entropy based solution to power meter placement. The idea here is to install each meter under consideration on a link i of the network which results in maximum reduction in overall network entropy. We consider all possible placement points for every meter to be placed and choose a link that reduce the network entropy to a minimum. Note that a reduction in network entropy is the sum of entropy reduction on the underlying link i and all other links whose entropy is minimized/reduced in effect of meter placement on link i.

In order to calculate the network entropy for every candidate link $l_{out}^{(d_o)}$, we first calculate the entropy of every link $l_{out}^{(d_i)}$ given $l_{out}^{(d_o)}$. These conditional entropies are efficiently calculated by multiplying $f_x(d_o)$ with transition functions of all devices on the path between links $l_{out}^{(d_o)}$ and $l_{out}^{(d_i)}$. We do not need to explicitly identify the path from $l_{out}^{(d_o)}$ to $l_{out}^{(d_i)}$ and we do not need to multiply the same transition functions again and again. The entropy calculation works in recursive fashion. Once we calculate

Algorithm 3: The MinEntropy Algorithm

Input: The topology T of the power grid; the pmf of the input feed to first device i.e., $f_x(0)$; transition functions $f(d)$; maximum number of meters M_{max}; and maximum uncertainty to allow δ_{max}

Output: L (list of devices to be selected for meter placement)

begin
  $M \leftarrow 0$; $\delta_{curr} \leftarrow \delta_{max}$;
  while *($M < M_{max}$ and $\delta_{curr} \geq \delta_{max}$)* **do**
    $maxReduction \leftarrow 0$;
    $selectedLink \leftarrow 0$;
    foreach *(device d in T)* **do**
      $entReduction \leftarrow$ calcNetworkEntropy(d);
      if $maxReduction < entReduction$ **then**
        $maxReduction \leftarrow entReduction$;
        $selectedLink \leftarrow d.outputLink$;
      end
    end
    L.add($selectedLink$);
    updateEntopies($selectedLink$);
    $\delta_{curr} \leftarrow \max(\mathcal{E})$; $M \leftarrow M + 1$;
  end
end

function calcNetworkEntropy(d) : *entRed*
begin
  F $\leftarrow$ identityMatrix(n);
  /* F is the combined transition function i.e., $f(d_i \mid d_o)$ */
  $d_o \leftarrow d$; $d_p \leftarrow d$; $d_i \leftarrow d$;
  entRed $\leftarrow$ recursiveConditional(d_0, d_p, d_i, F);
end

function recursiveConditional(d_o, d_p, d_i, F) : entRed
begin
  condEnt $\leftarrow$ - sum ($f(d_o) \times F \otimes \log(F)$);
  entRed $\leftarrow$ entropy(d_i) $-$ condEnt;
  foreach *(immediate child c of d_i)* **do**
    $F \leftarrow F \times f(c)$; /* child given parent link */
    /* for next recursive call, c is the inferred device and d_i is the previous device */
    $d_p \leftarrow d_i$; $d_i \leftarrow c$;
    if *($d_i \neq d_p$)* **then**
      entRed $\leftarrow$ entRed + recursiveConditional(d_o, d_p, d_i, F);
    end
  end
  $d_p \leftarrow d_i$; $d_i \leftarrow$ getParent(d_i);
  if *($d_i \neq -1$ and $d_i \neq d_p$)* **then**
    $F \leftarrow F \times f'(c)$; /* parent given child link */
    entRed $\leftarrow$ entRed + recursiveConditional(d_o, d_p, d_i, F);
  end
end

the conditional entropy for a directly connecting neighbor of $l_{out}^{(d_o)}$, we then recursively calculate the entropies of neighboring links of that neighbor. Here, it should be noted that 1) every link trigger the neighboring links except the one who triggered the link itself. So no infinite recursion takes place and every link is accessed only once; 2) The product of transition functions calculated from $l_{out}^{(d_o)}$ to some $l_{out}^{(d_k)}$ is used to calculate the next product; 3) if a link is invoking its parent link, we use reverse transition function $f'(d)$ of that device. Otherwise, the normal transition function $f(d)$ is used. After every meter placement, the link entropies are updated. The same process is repeated until all power quality meters are placed.

6.5 Evaluations

We evaluate the two algorithms on a set of simulated networks. The evaluation process is depicted in Fig. 6.3 where each algorithm is given the same network topology to place a set of M meters. The devices considered include bus, switch, transformer and UPS. Power quality events are assigned a number from 1-5 in order of severity in accordance with [25] where the lower number represents a clean input. These are listed in Table 6.1 along with their descriptions. Table 5.1 lists transition functions of various electrical components obtained from a real-world power quality dataset using our latent feature model. From the same dataset, we learn a prior on the utility feed of [0.9947 0.005 0.0002 0.00009 0.00001]. The algorithms we propose are generic and could be used for placing meters in other network configuration. We evaluate our algorithms on different topologies and network configurations including the IEEE 13-node distribution test feeder network. For the BP algorithm, we collect $N = 10000$ samples for each device using MC sampling. For each network configuration we place $M = 5$ meters in order of importance.

Figure 6.4 shows the meters placed by the two algorithms in various network topologies. The positions of the meters placed by both algorithms are essentially similar. The MinEntropy algorithm achieves much faster results, completing in less than a second in all cases. On the other hand, the BP takes a longer time to complete. This is because BP compares individual samples on all links for every possible placement while the MinEntropy approach computes the conditional entropies at unmetered locations using probability mass functions instead of using individual samples. Algorithm completion times for both BP and CE approaches are shown in Table 6.2.

Table 6.1: Event Types

Type	**Event Description**
1	Good/normal power quality.
2	Below 70% of nominal voltage for more than 0.02 seconds or below 80% of nominal voltage for more than 0.5 seconds.
3	Below 70% of nominal voltage for more than 0.2 seconds.
4	Interruption of at least 1 second.
5	Interruption of at least 5 minutes.

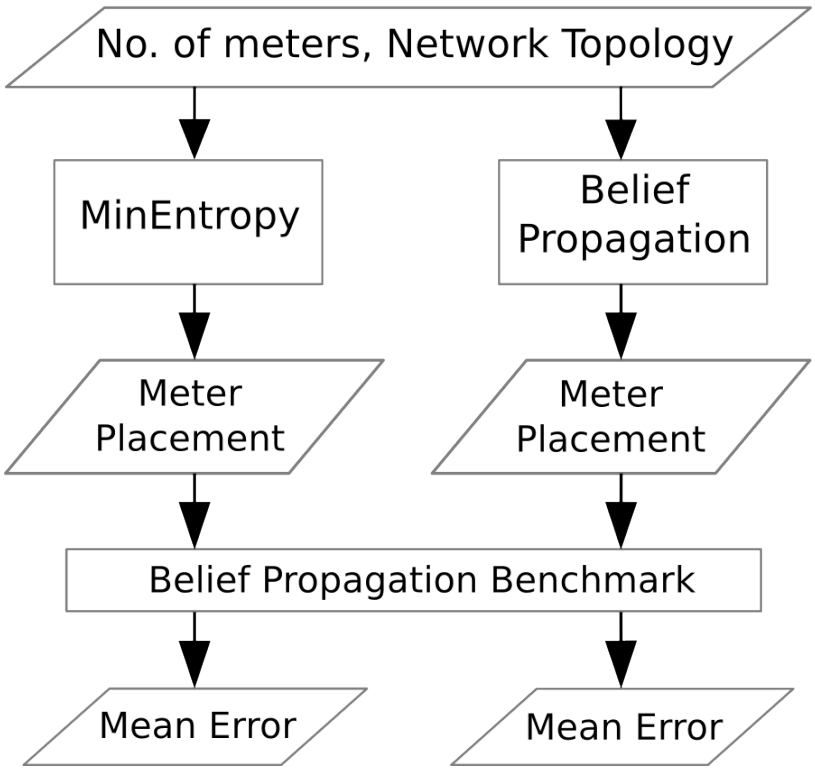

Figure 6.3: An overview of the meter placement evaluation process.

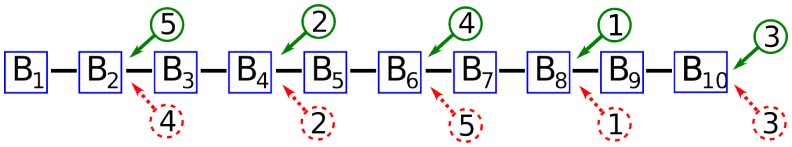

(a) Homogenous line network

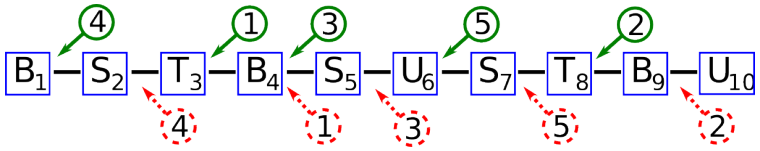

(b) Heterogeneous line network

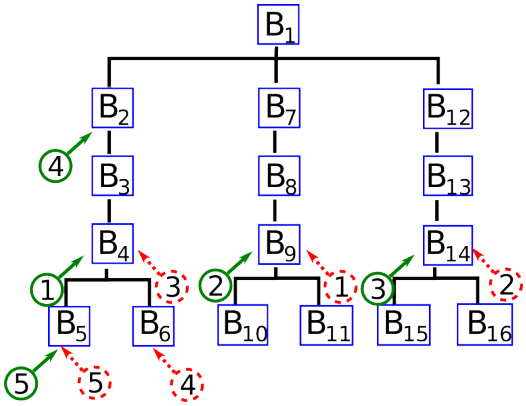

(c) Homogeneous tree network

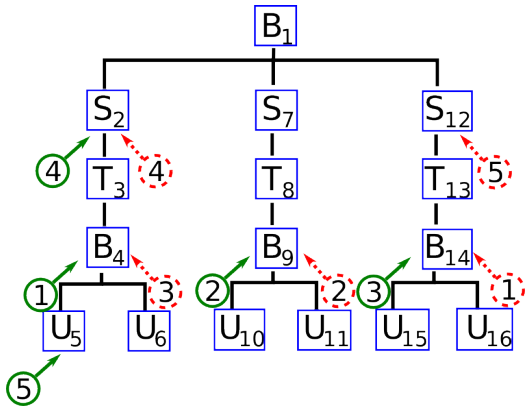

(d) Heterogeneous tree network

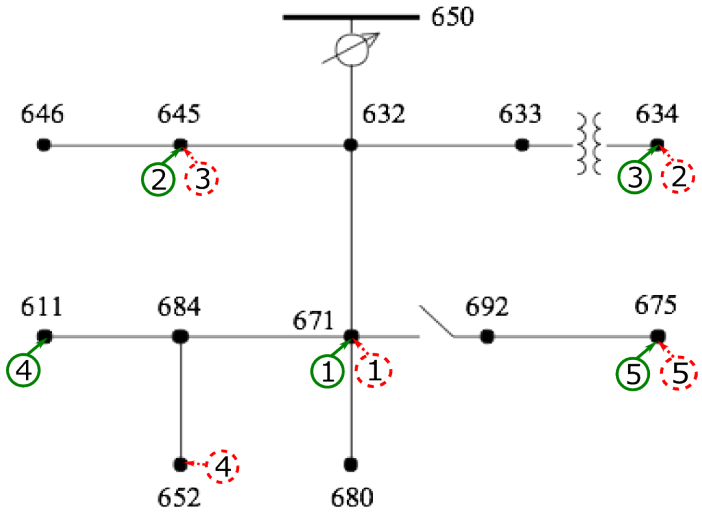

(e) IEEE 13-node distribution test feeder network

Figure 6.4: Networks used in our experiments. B=bus, S=switch, T=transformer, U=UPS. Ordered dotted circles correspond with the sequence of meters placed by BP while the solid circles show the meter placed by MinEntropy.

Table 6.2: Results for each network configuration

Network Topology	**Algorithm**	**Meter Placement Sequence**	**Mean Error Rate**	**Elapsed Time (seconds)**
Line homogeneous	BP	9,5,11,3,7	0.041112	270
	MinEnt	9,5,11,7,3	0.041112	0.064
Line heterogeneous	BP	5,10,6,3,8	0.040215	281
	MinEnt	4,9,5,2,7	0.064040	0.064
Tree homogeneous	BP	10,15,5,7,6	0.057893	727
	MinEnt	5,10,15,3,6	0.056891	0.138
Tree heterogeneous	BP	15,10,5,3,13	0.063510	727
	MinEnt	5,10,15,3,6	0.071655	0.138
IEEE 13-Node Test Feeder	BP	671,634,645,652,675	0.052381	802
	MinEnt	671,645,634,611,675	0.052381	0.138

Table 6.3: Number of meters required in various networks to restrict the mean error rate to 0.05 (5%).

Algorithm	**Line Homogen.**	**Line Heterogen.**	**Tree Homogen.**	**Tree Heterogen.**	**IEEE 13-Node Test Feeder**
BP	5	5	6	6	6
MinEnt	5	6	6	6	6
Random	7	8	8	8	8

The meter placements are then passed to the belief propagation benchmark to compare the accuracy of the two algorithms in terms of mean-square error (MSE), i.e., the mean error between the estimated and actual transition functions on unmonitored links. We collect a set of known samples for a given meter configuration and infer the maximum likelihood power quality event that would appear at each unmetered node using belief propagation. We then estimate the error rate for each node. If the inferred event differs from the event given by the MC sample, we add $1/N$ for that sample. The mean error rate across all nodes is taken as the final performance metric. As shown in Table 6.2, the MSEs are very small for both algorithms in all networks we tested. The BP algorithm gave slightly better estimations than MinEntropy in some cases at a cost of longer running times.

We also compare the accuracy of our algorithms in terms of cost savings. Table 6.3 shows the number of meters needed by each algorithm where it can be clearly seen that using our solution to achieve the same accuracy (error rate of < 0.05) can reduce the number of meters by 33%. Results of the Random placement algorithm were obtained by randomly placing meters until the desired accuracy was achieved.

6.6 Conclusion

Power quality meters are expensive devices and it is financially infeasible to install them on every link in the power network. We proposed algorithms which intelligently place power meters on selected power links to reduce the cost of power quality monitoring. We formulated the problem of selecting suitable meter placements in power networks such that power quality can be best predicted. Two approaches were presented, one based on conditional entropy and one considering prediction error. Experiments in various simulation networks including the IEEE 13-node distribution test feeder suggested that the conditional entropy based MinEntropy approach is much faster. Finally, the proposed solutions significantly reduce the uncertainty of power quality values on unmonitored power links.

Chapter 7

A Prediction Model

7.1 Motivation

As discussed in Chapter 1, the main objective of this work is to increase the reliability of power networks in terms of power quality within given financial budget/resources. In order to monitor the power quality, power quality meters are being deployed. Since power quality meters are expensive devices, we (in Chapter 5) proposed MaxEnt based algorithm for power quality estimation on unmonitored network segments. For meter placements, we proposed conditional entropy based efficient algorithms (in Chapter 6) that intelligently place power meters on selected network segments so that the power quality could be inferred as accurately as possible.

Since the power quality readings (exact readings from monitored links, and estimated PQ values from unmonitored links) are available now, we use these readings to estimate the state of the network and identify any potential malfunctioning device in the power network. Our objective in this chapter is to address the research challenge: *how to detect a potential malfunction device in the power network based on available power quality readings*. In this chapter, we propose a measure that helps to detect the malfunction devices in the power network. The simulation results confirm that the proposed solution is efficient, and accurate.

7.2 Problem Formulation

In this section, first we detail our assumptions of the problem domain and then formulate our research problem.

7.2.1 Assumptions

The four assumptions we make about the problem are as follows:

1. **The transfer function or behavior $\left(f\left(d\right)\right)$ of each device d in the network is known**. As discussed earlier, a device-specific power quality transfer function could be estimated through physical modeling or through the assessment of historical PQ data. In Chapter 3, using our real power quality dataset, we have demonstrated that how accurately the transfer function $f(d)$ could be estimated.

2. **All potential malfunction devices need to be on a monitored segment.** A potential malfunction device could effectively be detected when the device itself or any of its child device is monitored in real time using a PQ meter. This assumption is realistic in the sense that if the underline link is not monitored, we cannot get the real-time status of PQ values and would not be able to detect if a device is not behaving normally. On a monitored segment, the objective is to detect a device as a malfunction when that is significantly deviating form its normal behavior by producing bad power quality.

3. **The power grid network is a tree-structured network where the electric current flows from root node to the child nodes.** As discussed in Chapter 6, this is a reasonable assumption at any particular instance in time. While enterprise level power grids used in places such as hospitals and data centers often have two utility feeds available as well as an independent emergency power source, only one power source is typically used at one time. See the IEEE Gold Book [9] for further information on recommended practices in the design of critical power systems.

4. **The probability mass function $\left(f_x\left(d_0\right)\right)$ of power quality values at the input link to the root node is known.** In other words, the distribution of power quality at the input to the network, usually the utility feed, is known. This is also a reasonable assumption, since electrical utilities typically report on indices such as System Average RMS Variation Frequency Index (SARFI) which is essentially a count of the number of times the magnitude and duration falls below a threshold. Furthermore, there are often independent bodies that gather statistics on power delivery service reliability that can also be incorporated into an estimate of power quality distribution [24].

7.2.2 The Problem

We now formulate the problem of detecting a malfunction device in the network. The objective is to detect a device d in the network as a malfunction device when its power quality output degrades persistently from its normal/actual behavior. Since the transition function $f(d)$ of each device d is known, we know the probability distribution of the output power quality ($f_x(d)$) at the output link of each device in the power grid network. Figure 7.1 shows the probability distributions for various devices in a sample network. The distributions are obtained/computed for the prior distribution of [0.9947 0.005 0.0002 0.00009 0.00001] at the utility feed/generator.

We mathematically analyze these distributions and based on their various statistical properties, we propose out detection algorithm in the next section. The proposed algorithm compares the normal behavior ($f_x(d)$) of each device with the observed behavior ($\overset{\circ}{f}_x(d)$) and compute the power quality degradation (the difference between the two distributions) as Δ_d . The objective function becomes:

$$\Delta_d = f_x(d) \overset{\triangleq}{\leftrightarrow} \overset{\circ}{f}_x(d) \tag{7.1}$$

where the operation $\overset{\triangleq}{\leftrightarrow}$ is unknown. In the next section, we propose algorithms to solve the equation 7.1.

7.3 Our Detection Algorithms

7.3.1 A Simple Correlation Measure

To compare two probability distributions, the correlation measure is usually used where its most familiar type is the *Pearson's correlation coefficient*, simply known as *the correlation coefficient*. In order to use the formula, we represent the actual PQ distribution as X while the obtained distribution as Y. For the random variables X and Y, it is defined as:

$$\rho_{X,Y} = corr(X,Y) = \frac{\sum(x-\bar{x})(y-\bar{y})}{\sqrt{\sum(x-\bar{x})^2 \sum(y-\bar{y})^2}}$$

The above correlation measure could be used to compare the actual and observed PQ distributions. Generally speaking, this measure can accurately tell how much the observed distribution is similar to (or different from) the actual distribution of

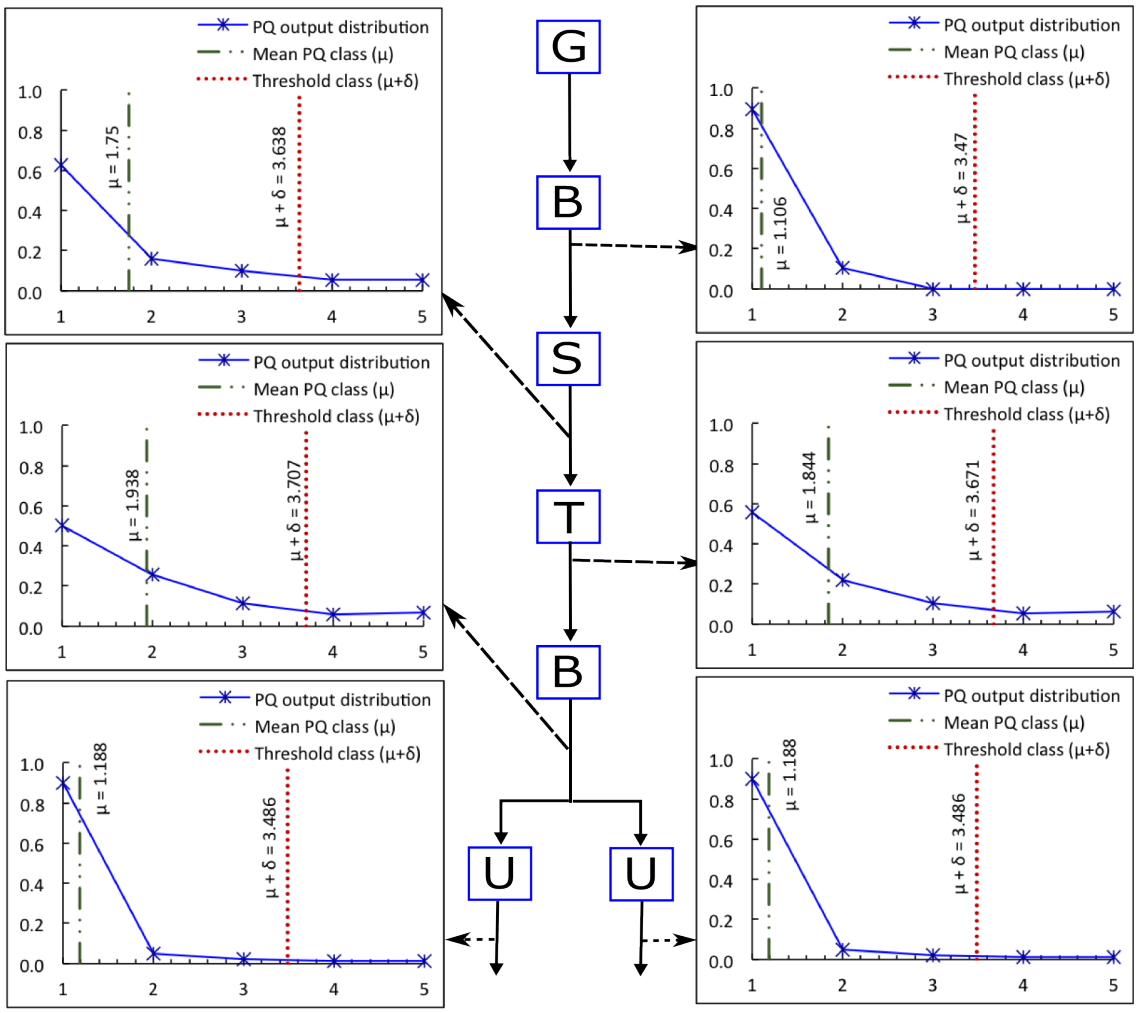

Figure 7.1: Power quality distributions and their average output power quality class for various devices. The average power quality class and computed threshold is shown as vertical lines in each distribution graph. The x-axis represents the power quality class c_i while the y-axis represents the probability of c_i. Further, the lower class c_1 represents the best power quality while c_5 represents the worst power quality.

the same device. When a device is perfectly behaving like its actual distribution, the measure returns a maximum value (+1). On the other hand, when a device is producing a very different distribution (for instance producing very bad PQ), it returns a smaller value (the smallest possible is -1). The value 0 (or closer to 0) represents that the two distributions have no correlation, i.e., they are asymmetric. Although this technique is simple to use, we found various scenarios where it is not able to accurately detect the power quality degradation. We classify the identified scenarios in two classes: 1) a malfunction device is not detected; and 2) a better PQ producing device is classified as a malfunction. Both cases are explained as follows.

Missed Detection Scenarios

This scenario arises when a device is producing a very bad power quality (malfunction device) and the system does not detect it. This measure classifies the observed distribution as perfectly normal (similar to the actual) when the correlation is a +1 (or close to +1). For all normal behaving devices, the observed distribution will be very similar to the actual and a +1 correlation will perfectly classifying them as normal. Nevertheless, we identified cases where the PQ is significantly degraded and the distributions were still highly correlated. In all those cases, we cannot use this simple correlation measure. Figure 7.2a shows one such example where the power quality is significantly degraded (the dotted line) and the correlation coefficient is still very high (a +1).

False Detection Scenarios

We call it a false detection when a device that is generating similar or slightly different (good or bad) power quality output than its normal and classified as a malfunction. Using the correlation measure, a device is detected as malfunction when the correlation coefficient is negative or (closer to 0). Although we observed that this measure works in various cases, we have been able to identify few scenarios where the simple correlation measure will not work. These scenarios are explained under two categories as follows:

1. **Zero correlation:** A zero correlation means the two distributions do not share any particular correlation. In our case, most probably, observing a distribution which do not share any correlation with its actual distribution implies the degradation in the power quality. Nevertheless, based on the correlation measure only,

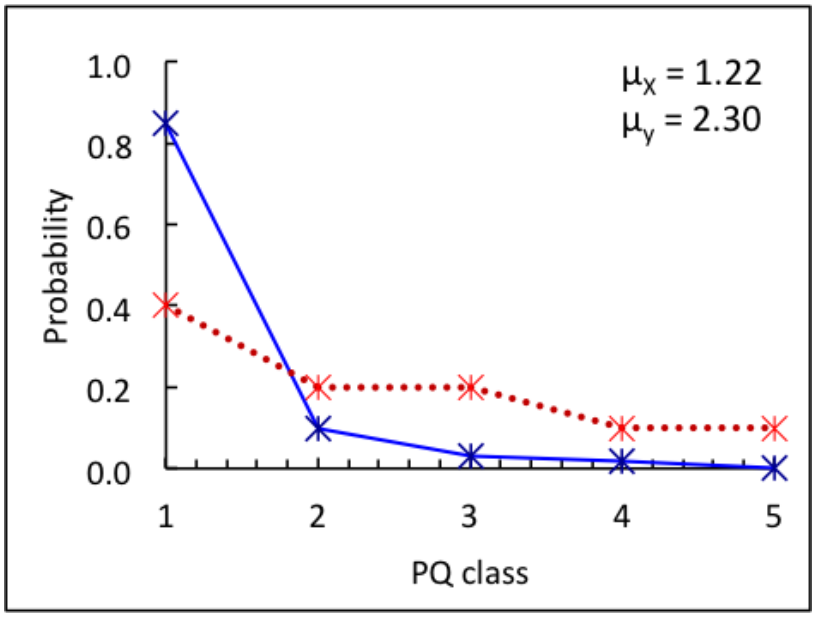

(a) Positive correlation ($\rho_{X,Y} = +0.95 \approx +1$)

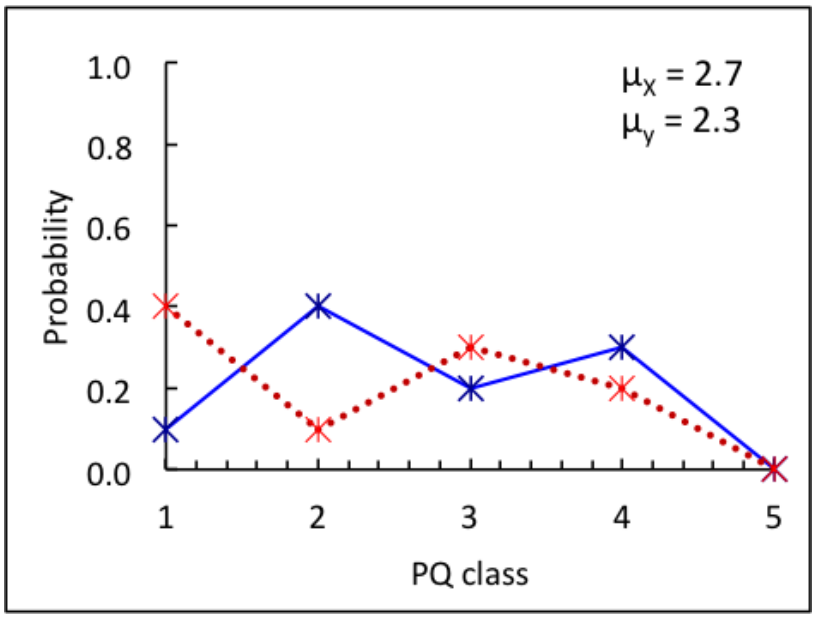

(b) Zero correlation ($\rho_{X,Y} = 0$)

Figure 7.2: Positive correlation scenarios where the simple correlation technique is not useful.

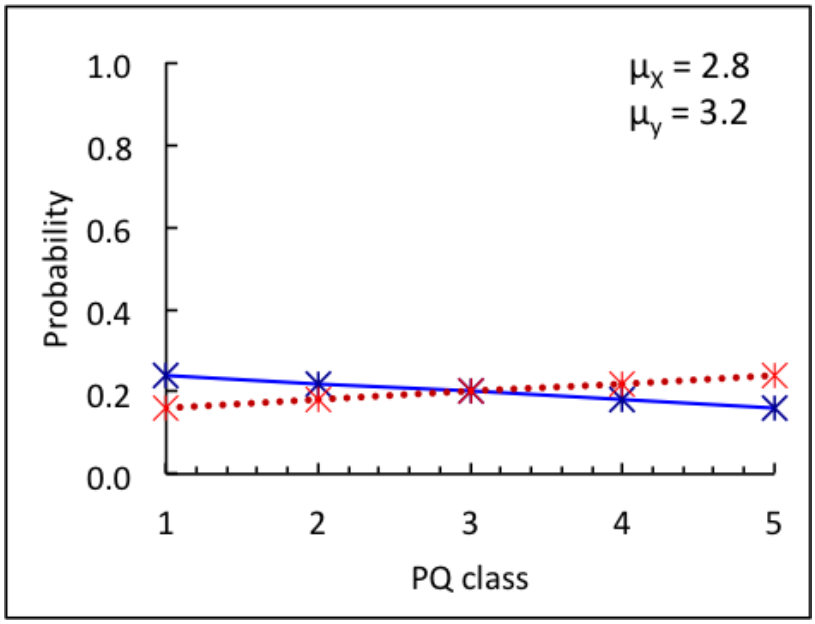

(a) Negative correlation ($\rho_{X,Y} = -1$)

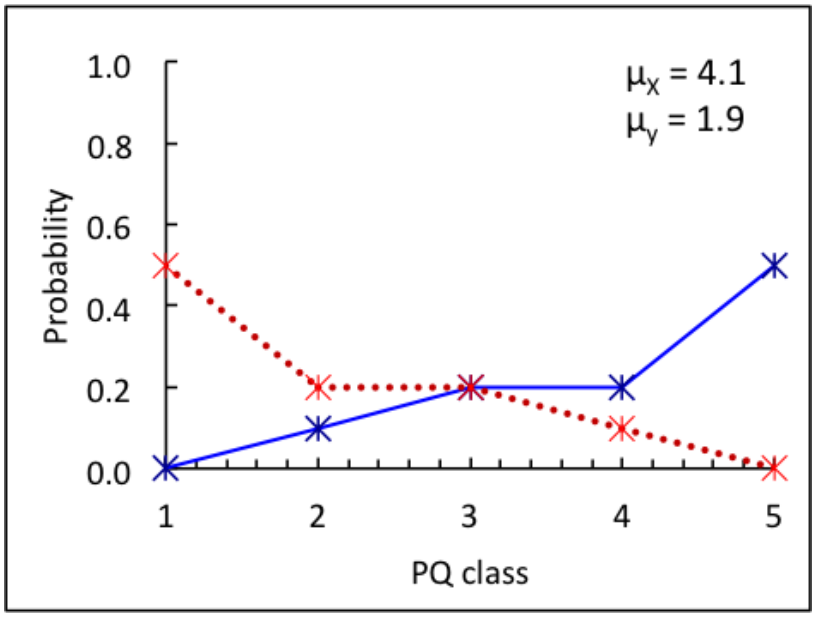

(b) Negative correlation ($\rho_{X,Y} = -1$)

Figure 7.3: Negative correlation scenarios where the simple correlation technique is not useful.

we cannot tell for sure if the observed (and non-correlated) distribution is better or worse than its actual distribution in terms of power quality. Figure 7.2b represents a scenario where the observed power quality is better than its actual expected behavior. In such cases, simply based on a zero correlation, we cannot classify those devices as malfunction.

2. **Negative correlation:** In a negative correlation between two variables, the value of one variable increases when the other decreases, and vice versa. Although theoretically possible, it is rare to get a perfectly negative correlation in power quality measures. In a negative correlation, the observed distribution is either bad or good compared to the actual distribution. Although the probability of getting a bad PQ is higher than that of a good, it cannot always be guaranteed. Further, the negative correlation can quantify the symmetry of two distributions, it cannot essentially quantify how much the distributions are different in terms of power quality degradation. For instance, Figure 7.3a shows a 100% negative correlation (with coefficient of -1) but the actual PQ degradation is very minor. Finally, as another evidence, we in Figure 7.3b demonstrates a significant PQ improvement with a correlation of -1.

7.3.2 An Expected Value Based PQ Measure

This measure is based on measuring the average power quality output over a period. A device is classified as a malfunction if its observed PQ output significantly degrades from its actual average power quality output. Clearly, if a device starts to malfunction by producing bad PQ output, its average output will deviate from its actual average output. We measure this deviation as Δ_d and is computed as follows.

$$\Delta_d = E[f_x(d)] - E[\overset{\circ}{f}_x(d)] \leq \theta_d$$

where θ_d is the threshold/maximum value allowed at which a device is classified as malfunction. In other words, θ_d is the maximum allowed deviation between the expected PQ classes of the two distributions. The value of θ_d could be fixed for all devices. For instance, by using $\theta_d = 1$, any device whose average output degrades by 1 PQ class from its actual average output will be classified as a malfunction device. We use θ_d equal to the standard deviation of the actual output distribution, i.e., $\theta_d = \sigma_d$. Using standard deviation as threshold will allow us to use slightly larger/relaxed

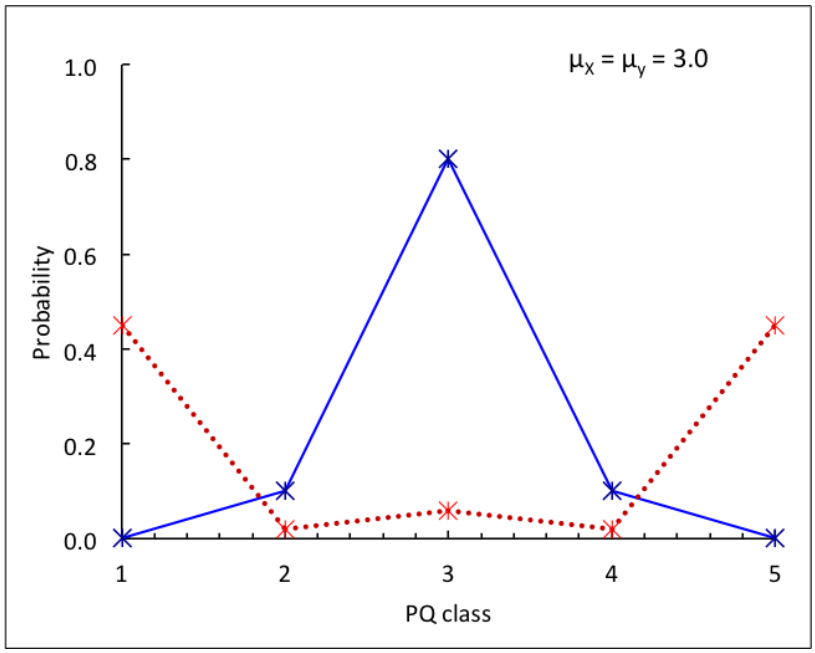

Figure 7.4: Two very different power quality distributions with same expected/average PQ output/class.

threshold for devices generating less uncertain outputs in normal conditions (compared to other devices in the same network). Figure 7.1 shows the expected value and corresponding threshold values for various devices in our sample power grid.

The proposed measure is simple and accurately detects malfunction devices in the network. On the contrary, it is theoretically possible to produce two very different PQ distributions with same average/expected value. One such scenario is demonstrated in Figure 7.4 where two very different power quality output distributions have exact same expected output PQ class. Since, on average, the two distributions in Figure 7.4 represents the same power quality, it is debatable whether the observed distribution is better or worse than its normal. We take a safer approach and address the problem by proposing a composite measure as follows.

7.3.3 A Composite Measure

As discussed earlier, we know that the average power quality degrades (to a higher PQ class) when a devices produce significantly bad power quality than its actual power quality. Simply measuring the difference between the expected values of the actual, and observed PQ classes can accurately detect a malfunction device. Although this simple technique works well, theoretically it is possible that a very different observed PQ output may produce similar expected values. To address this problem, we propose a composite expected value measure that enhances the accuracy of detecting a malfunction device in terms of power quality degradation.

In the composite expected value measure, we calculate two different expected values: 1) expected value of the complete distribution; and 2) expected value of the PQ classes greater than the average class computed on complete distribution (all classes). This composite measure increases the accuracy of our detection solution. In other words, for a malfunction device, if the observed expected value is similar to the actual expected value, the probability values of the higher classes must be greater (or the device is not a malfunction). Our proposed algorithm is shown as Algorithm 4. The main steps in the algorithms are described as follows.

1. **Input parameters:** The proposed algorithm requires these parameters: 1) network topology, 2) metered locations, 3) device transfer functions $f(d)$, 4) prior distributions $f_x(d_0)$, and 5) size of the sliding size w that represents the number of PQ readings to use for computing our composite measure. Further,

Algorithm 4: A malfunction device detection algorithm

Input: distribution function of input link to device 1 i.e., $f_x(0)$, transfer function $f(d)$, network topology T, set of positions of the installed power meters M

Output: L (list of devices detected as malfunction)

begin

/* One time parameter computations */

foreach *(Device d in level order)* **do**

$parent \leftarrow$ getParent(d); $f_x(d) \leftarrow f_x(parent) \times f(d)$;

$\mu_f^d \leftarrow$ computeFullMean$(f_x(d))$; $\mu_p^d \leftarrow$ computePartialMean$(f_x(d), \mu_f^d)$;

$\sigma_f^d \leftarrow$ computeFullSDev$(f_x(d))$; $\sigma_p^d \leftarrow$ computePartialSDev$(f_x(d), \mu_f^d)$;

end

/* Every meter records a PQ events $e_d^{(t)}$ continuously (usually every few seconds)

$e_d = [e_d^{(1)}, e_d^{(2)}, \ldots, e_d^{(w)}]$ is the set of PQ recordings for a metered device d */

foreach *(Time Interval t)* **do**

foreach *(Metered Device d)* **do**

/* get latest W readings for each metered device d */

$e_d \leftarrow$ getLastestReadings(w, d);

$\mu_F \leftarrow$ computeFullMean(e_d);

$\mu_P \leftarrow$ computePartialMean(e_d, μ_f^d);

if *(*$((\mu_F - \mu_f^d) > \sigma_f^d \;||\; (\mu_p - \mu_p^d) > \sigma_p^d)$ **then**

L.add(d);

end

end

end

end

we compute the actual standard deviation of each device σ_d from the actual output distributions.

2. **PQ readings from metered locations:** The installed power quality meters measure send the power quality reading to a central location. Our algorithm continuously reads these recordings/readings.

3. **Computing Δ_d:** In order to compute the Δ_d, we need the actual and observed expected values. The expected values of the actual distributions are computed only once while while the observed values are computed periodically using new PQ reading in that interval.

4. **Device classification:** Periodically after a fixed interval t, the algorithm compares the observed expected values (both and full partial) and classifies a device d as malfunction if any of the observed measures exceeding by θ_d from its actual expected values.

7.4 Evaluations

7.4.1 Simulation setup

We simulate the power grid network in MATLAB. The inputs include: 1) Network topology as an adjacency matrix, 2) device type (e.g., bus, switch, UPS, transformer etc) of each node, 3) transfer matrix $f(d)$ for each node d, 3) PQ distribution vector $f_x(d_0)$ of the utility feed, and 4) vector of metered locations.

The power quality events were generated using the input distribution $f_x(d_0)$, and transfer function $f(d)$ in level order starting from the root node of the tree. A power quality event e_d at a node d is generated based on the event at its parent link ($e_{\hat{d}}$). For example a PQ event of class c_3 at a parent link will result into a child event following the distribution in 3^{rd} row of $f(d)$. Since the transfer matrices $f(d)$ are computed using our real PQ dataset (see Chapter 3), the simulated events possesses similar statistical features.

We select a device d in the start of our simulation as a malfunction device and modify its transfer function from $f(d)$ to a malfunction transfer function $\acute{f}(d)$. The objective is to detect the effect of a malfunction device at the following metered location. The process was repeated for all devices by infecting one device at a time.

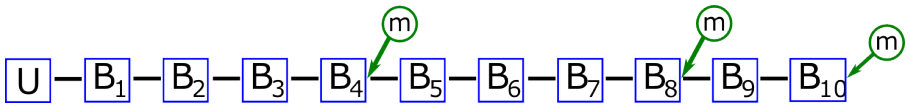

(a) Homogenous line network

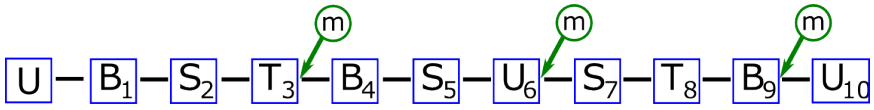

(b) Heterogeneous line network

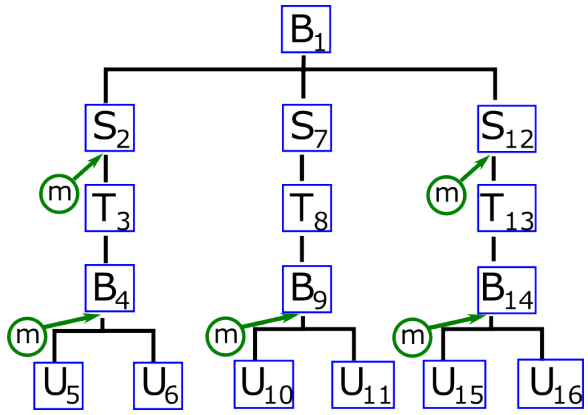

(c) Heterogeneous tree network

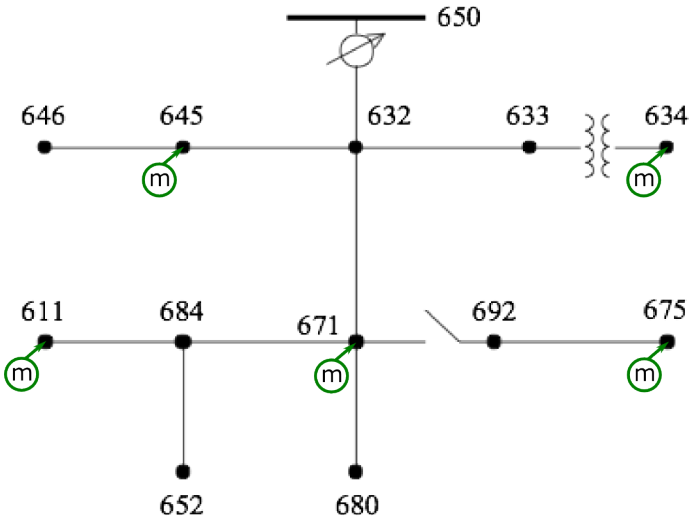

(d) IEEE 13-node distribution test feeder network

Figure 7.5: Networks used in our experiments. B=bus, S=switch, T=transformer, U=UPS. The circled m indicates the position of a meter. The meter positions are based on our meter placement solution proposed in Chapter 6.

For a malfunction device, we use a uniform transfer function, e.g., for five event types, the transfer function is

$$\acute{f}(d) = \begin{bmatrix} 0.2 & 0.2 & 0.2 & 0.2 & 0.2 \\ 0.2 & 0.2 & 0.2 & 0.2 & 0.2 \\ 0.2 & 0.2 & 0.2 & 0.2 & 0.2 \\ 0.2 & 0.2 & 0.2 & 0.2 & 0.2 \\ 0.2 & 0.2 & 0.2 & 0.2 & 0.2 \end{bmatrix}.$$

Experimental results on various network types are discussed next.

7.4.2 Simulation results

Figure 7.5 show various network types used in our simulation to evaluate the accuracy of our proposed solution. The metered position are obtained using our meter placement solution from Chapter 6. We evaluated all 4 networks for all devices that are on monitored segments and the algorithm correctly identified the malfunction segment.

7.5 Conclusion

Power quality meters play an important role in the reliability of power networks. Using power quality reading from the metered locations in the network, we proposed statistical measures that help in accurately detecting a malfunction segment in the power network. The proposed solution was evaluated on various types of networks including the IEEE Test Feeder network. Our experimental evaluations confirm the accuracy of the proposed solution. Further, the malfunction segment detection will help in the reliability of power networks.

Chapter 8

Conclusions and Future Work

Power quality plays an important role in the reliability of power grids. To improve the reliability of the power grid networks, power quality (PQ) measurement devices are being deployed to monitor the power quality on underlying links. Since power quality meters are expensive devices, it is financially infeasible to install them on every link between devices in the power grid network. In the first part of this thesis, we studied the problem of estimating the power quality on unmonitored network segment based on power quality readings from the monitored segments. We modeled the power grid network as a data network to leverage the existing network and data estimation techniques to solve the problem. To solve the power quality estimation on unmonitored links, we proposed a maximum entropy (MaxEnt) based model that accurately estimates power quality transition functions. Through experimental evaluations, we showed that our MaxEnt based solution is much faster and accurate than the existing expectation maximization (EM) based solution.

Next, we investigated the problem of intelligently placing measurement devices on suitable power links to reduce the uncertainty of PQ estimation on unmonitored power links. As a first step to tackle the meter placement challenge, we represented the latent feature of a device as a transition function which is usually estimated through physical modeling or through the assessment of historical power monitoring data. Using a real PQ dataset, we showed that historical data can be used to capture the latent features of a device. After learning the device latent features, we then proposed intelligent meter placement algorithms for identifying network segments suitable for power meter placement. The two algorithms that solve the meter placement problem are: 1) an intelligent conditional entropy (CE)-based algorithm; and 2) a Bayesian network (BN)-based approach. The two algorithms were evaluated in

various simulation networks including the IEEE 13-node distribution test feeder. Results suggested that the CE-based MinEntropy approach is much faster. Further, the proposed solutions significantly reduced the uncertainty of PQ values on unmonitored power links.

Finally, using the power quality readings/events from monitored segments, we identified statistical features and proposed a model that accurately identify a potential malfunction device in the power network. The proposed solution was evaluated on various simulated power networks including the IEEE Test Feeder network. Our evaluations confirmed the accuracy of the proposed solution. The proposed malfunction segment detection solution will help in the reliability improvement of power networks.

8.1 Future Work

8.1.1 Scaling the MaxEnt-based PQ Estimation

Our proposed MaxEnt-based model opens a new scope of methods to quantitatively measure and solve the reliability problems in smart grid. The proposed solution may not converge efficiently for sub-nets of larger sizes. The scalability problem arises as the number of unknown variables increases exponentially with the increase in the number of components in a subnet. The idea for the extended work is to divide the larger subnets in logical components where each logical component will represent several physical components. Instead of computing individual transfer functions for each physical device, transfer functions of the logical components could be estimated first. In the second round, transfer functions of individual physical components could be estimated from the logical transfer functions. Note that this is a high level guideline which only serves as a starting point towards the final solution. The final solution could be based on a comprehensive mathematical model. Finally, for the evaluation of such a system, various larger IEEE standard test networks could be used.

8.1.2 Extending the Meter Placement Solution to Larger Networks that Contain Loops

Our meter placement solution could be used for meter placement in several standard power networks including the 13-Node IEEE Test Feeder. As a future work, one could look into the possibility of extending our work to cover the networks that contain loops

to relax our tree network assumption.

8.1.3 Device Level Misbehavior Detection

In this thesis, we have proposed statistical measures that help in detecting a potential malfunction device in the power network. If the device is not directly monitored, e.g., it is somewhere in the middle of a monitored segment, we can only detect the segment and not the device explicitly. As a future work, the solution could be improved to detect the malfunction device explicitly that is not directly monitored. Further, it could also be investigated if the accumulative suffer time of the device (using the standard measures defined in the CBEMA curve) could be used to make the device maintenance/replacement recommendations.

Chapter 9

Publications

1. **Sardar Ali**, Kui Wu, Kyle Weston, and Dimitri Marinakis, "A Machine Learning Approach to Meter Placement for Power Quality Estimation in Smart Grid," Accepted by *IEEE Transactions on Smart Grid (TSG)*.

2. **Sardar Ali**, Kyle Wetson, Dimitri Marinakis, and Kui Wu, "Intelligent Meter Placement for Power Quality Estimation in Smart Grid," *IEEE SmartGridComm*, Vancouver, Canada, 2013.

3. **Sardar Ali**, Kui Wu, and Dimitri Marinakis, "A maximum-Entropy Based Fast Estimation of Power Quality for Smart Microgrid," *IEEE SmartGridComm*, Vancouver, Canada, 2013.

Bibliography

[1] IEC, "Electromagnetic compatibility (emc) - part 2: Environment - section 5: Classification of electromagnetic environments," *IEC/TS 61000-2-5*, 1995.

[2] IEEE, "IEEE recommended practice for monitoring electric power quality," *IEEE Std 1159-2009 (Revision of IEEE Std 1159-1995)*, pp. c1–81, June 2009.

[3] K. Moslehim and R. Kumar, "A reliability perspective of the smart grid," *IEEE TRANSACTIONS ON SMART GRID*, vol. 1, june 2010.

[4] R. Albert, I. Albert, and G. L. Nakarado, "Structural vulnerability of the North American power grid," *Phys. Rev. E*, vol. 69, Feb 2004.

[5] Fluke Corporation, "Fluke Power Quality Analyzers." `http://www.fluke.com/fluke/usen/products/categorypqttop.htm`. [Online: accessed Aug. 2013].

[6] Schneider Electric, "PowerLogic Energy and Power Quality Meters." `http://www.schneider-electric.com`. [Online: accessed Aug. 2013].

[7] E. T. Jaynes, "Information theory and statistical mechanics," *The Physical Review*, vol. 106, no. 4, pp. 620–630, 1957.

[8] ITI, "ITI (CBEMA) Curve Application Note," tech. rep., Information Technology Industry Council (ITI), October 2007.

[9] IEEE, "IEEE recommended practice for the design of reliable industrial and commercial power systems," *IEEE Std 493-2007 (Revision of IEEE Std 493-1997)*, pp. 1–383, 2007.

[10] C. Gamroth, K. Wu, and D. Marinakis, "A smart meter based approach to power reliability index for enterprise-level power grid," in *Smart Grid Communications (SmartGridComm), 2012 IEEE Third International Conference on*, pp. 534–539, IEEE, 2012.

[11] K. D. McBee and M. G. Simoes, "Utilizing a smart grid monitoring system to improve voltage quality of customers," *IEEE Trans. Smart Grid*, vol. 3, no. 2, pp. 738–743, 2012.

[12] C. F. M. Almeida and N. Kagan, "Harmonic state estimation through optimal monitoring systems," *IEEE Trans. Smart Grid*, vol. 4, no. 1, pp. 467–478, 2013.

[13] M. Savaghebi, A. Jalilian, J. C. Vasquez, and J. M. Guerrero, "Secondary control for voltage quality enhancement in microgrids," *IEEE Trans. Smart Grid*, vol. 3, no. 4, pp. 1893–1902, 2012.

[14] A. Farzanehrafat and N. R. Watson, "Power quality state estimator for smart distribution grids," *IEEE Trans. Power Systems*, vol. 28, no. 3, pp. 2183–2191, 2013.

[15] S. G. Ghiocel, J. H. Chow, G. Stefopoulos, B. Fardanesh, D. Maragal, B. Blanchard, M. Razanousky, and D. B. Bertagnolli, "Phasor-measurement-based state estimation for synchrophasor data quality improvement and power transfer interface monitoring," *IEEE Trans. Power Systems*, vol. 29, no. 2, pp. 881–888, 2014.

[16] A. Krause and C. Guestrin, "Optimizing Sensing from Water to the Web," *IEEE Computer Magazine*, August 2009.

[17] W. Yuill, A. Edwards, S. Chowdhury, and S. P. Chowdhury, "Optimal PMU placement: a comprehensive literature review," in *IEEE Power and Energy Society General Meeting*, (Detroit, Michigan), July 2011.

[18] J. Chen and A. Abur, "Placement of pmus to enable bad data detection in state estimation," *IEEE Trans. Power Systems*, vol. 21, no. 4, pp. 1608–1615, 2006.

[19] R. Singh, B. C. Pal, R. A. Jabr, and R. B. Vinter, "Meter placement for distribution system state estimation: an ordinal optimization approach," *IEEE Trans. Power Systems*, vol. 26, no. 4, pp. 2328–2335, 2011.

[20] M. Shahraeini, M. S. Ghazizadeh, and M. H. Javidi, "Co-optimal placement of measurement devices and their related communication infrastructure in wide area measurement systems," *IEEE Trans. Smart Grid*, vol. 3, no. 2, pp. 684–691, 2012.

[21] J. Liu, J. Tang, F. Ponci, A. Monti, C. Muscas, and P. A. Pegoraro, "Trade-offs in pmu deployment for state estimation in active distribution grids," *IEEE Trans. Smart Grid*, vol. 3, no. 2, pp. 915–924, 2012.

[22] J. Pearl, *Probabilistic Reasoning in Intelligent Systems: Networks of Plausible Inference*. Morgan Kaufmann Pub, 1988.

[23] J. S. Yedidia, W. T. Freeman, Y. Weiss, *et al.*, "Generalized belief propagation," *Advances in neural information processing systems*, pp. 689–695, 2001.

[24] A. Chowdhury, T. Mielnik, L. Lawion, M. Sullivan, and A. Katz, "Reliability worth assessment in electric power delivery systems," in *Power Engineering Society General Meeting, 2004. IEEE*, pp. 654–660, IEEE, 2004.

[25] EPRI, "Analysis of extremely reliable power delivery systems: A proposal for development and application of security, quality, reliability, and availability (sqra) modeling for optimizing power system configurations for the digital economy," *CEIDS*, 2002.